NAVAL POSTGRADUATE SCHOOL

MONTEREY, CALIFORNIA

THESIS

OPTIMAL SUPER DIELECTRIC MATERIAL

by

Natalie-Rose L. Jenkins

September 2015

Thesis Advisor: Jonathan Phillips
Co-Advisor: Young Kwon

THIS PAGE INTENTIONALLY LEFT BLANK

REPORT DOCUMENTATION PAGE

Form Approved OMB No. 0704–0188

1. AGENCY USE ONLY *(Leave blank)*	**2. REPORT DATE** September 2015	**3. REPORT TYPE AND DATES COVERED** Master's Thesis

4. TITLE AND SUBTITLE
OPTIMAL SUPER DIELECTRIC MATERIAL

5. FUNDING NUMBERS
RPJY3
W4P06

6. AUTHOR(S) Jenkins, Natalie-Rose L.

7. PERFORMING ORGANIZATION NAME(S) AND ADDRESS(ES)
Naval Postgraduate School
Monterey, CA 93943–5000

8. PERFORMING ORGANIZATION REPORT NUMBER
N/A

9. SPONSORING /MONITORING AGENCY NAME(S) AND ADDRESS(ES)
Navy Energy Coordination Office(N-4)
Expeditionary Energy Office-3000 Marine Corps, Pentagon, Room 2C252A
Washington D.C. 20350-1775

10. SPONSORING/MONITORING AGENCY REPORT NUMBER
N/A

11. SUPPLEMENTARY NOTES The views expressed in this thesis are those of the author and do not reflect the official policy or position of the Department of Defense or the U.S. Government. IRB Protocol number ____N/A____.

12a. DISTRIBUTION / AVAILABILITY STATEMENT
Approved for public release; distribution is unlimited

12b. DISTRIBUTION CODE

13. ABSTRACT (maximum 200 words)

The results of this study establish that powder-based super dielectric materials (SDM) are a large family of porous electrically insulating materials filled to the point of incipient wetness (paste consistency) with liquids containing dissolved ions. This work studied the dielectric behavior at low frequency of four different high surface area, porous, refractory oxides: two alumina materials, one silica, and one fumed silica, filled with aqueous solutions containing one of two salts (NaCl or NH4Cl). All were found to have dielectric constants greater than 10^9. This strongly supports the fundamental hypothesis of SDM: In the presence of an electric field any electrically insulating, porous material containing liquid with dissolved ionic species will form large dipoles, polarized opposite the applied field. Large dipole SDM placed between the electrodes of a parallel plate capacitor will reduce the net field to an unprecedented extent.

This family of materials can form materials with dielectric values orders of magnitude greater than any material previously studied (ca. 10^4 BaTiO3). Moreover; this study establishes that the identity of the porous insulating media can greatly impact the dielectric constant; 10^9 alumina; 10^{11} fumed silica. One implication of these results is that SDM can potentially be optimized to create capacitors with unprecedented energy density.

14. SUBJECT TERMS
capacitor, supercapacitor, super dielectric material

15. NUMBER OF PAGES
73

16. PRICE CODE

17. SECURITY CLASSIFICATION OF REPORT	**18. SECURITY CLASSIFICATION OF THIS PAGE**	**19. SECURITY CLASSIFICATION OF ABSTRACT**	**20. LIMITATION OF ABSTRACT**
Unclassified	Unclassified	Unclassified	UU

NSN 7540–01–280–5500

Standard Form 298 (Rev. 2–89)
Prescribed by ANSI Std. 239–18

THIS PAGE INTENTIONALLY LEFT BLANK

Approved for public release; distribution is unlimited

OPTIMAL SUPER DIELECTRIC MATERIAL

Natalie-Rose L. Jenkins
Lieutenant, United States Navy
B.S., United States Naval Academy, 2009

Submitted in partial fulfillment of the
requirements for the degree of

MASTER OF SCIENCE IN MECHANICAL ENGINEERING

from the

NAVAL POSTGRADUATE SCHOOL
September 2015

Author: Natalie-Rose L. Jenkins

Approved by: Jonathan Phillips, PhD
Thesis Advisor

Young Kwon, PhD
Co-Advisor

Garth Hobson, PhD
Chair, Department of Mechanical and Aerospace Engineering

THIS PAGE INTENTIONALLY LEFT BLANK

ABSTRACT

The results of this study establish that powder-based super dielectric materials (SDM) are a large family of porous electrically insulating materials filled to the point of incipient wetness (paste consistency) with liquids containing dissolved ions. This work studied the dielectric behavior at low frequency of four different high surface area, porous, refractory oxides: two alumina materials, one silica, and one fumed silica, filled with aqueous solutions containing one of two salts (NaCl or NH_4Cl). All were found to have dielectric constants greater than 10^9. This strongly supports the fundamental hypothesis of SDM: In the presence of an electric field any electrically insulating, porous material containing liquid with dissolved ionic species will form large dipoles, polarized opposite the applied field. Large dipole SDM placed between the electrodes of a parallel plate capacitor will reduce the net field to an unprecedented extent.

This family of materials can form materials with dielectric values orders of magnitude greater than any material previously studied (ca. 10^4 BaTiO3). Moreover; this study establishes that the identity of the porous insulating media can greatly impact the dielectric constant; 10^9 alumina; 10^{11} fumed silica. One implication of these results is that SDM can potentially be optimized to create capacitors with unprecedented energy density.

THIS PAGE INTENTIONALLY LEFT BLANK

TABLE OF CONTENTS

LIST OF FIGURES

THIS PAGE INTENTIONALLY LEFT BLANK

LIST OF TABLES

THIS PAGE INTENTIONALLY LEFT BLANK

LIST OF ACRONYMS AND ABBREVIATIONS

CED	composite electrolyte dielectric
cm	centimeter
EDLC	electric double-layer capacitor
EDS	energy dispersive X-ray spectroscopy
F	farads
J	joules
HSA	high surface area
kΩ	kiloohms
LAWS	Laser Weapon system
LSPSDA	Laser Scattering Particle Size Distribution Analyzer
m	meter
MLCC	multi-layer ceramic capacitor
mm	millimeter
nF	nanofarad
NPS	Naval Postgraduate School
MW	megawatts
RC	resistor/capacitor
SDM	super dielectric material
SEM	scanning electron microscopy
UAV	unmanned aerial vehicles
V	volts

THIS PAGE INTENTIONALLY LEFT BLANK

ACKNOWLEDGMENTS

I would like to thank my advisor, Professor Jonathan Phillips, for his support and guidance over this last year. I appreciate his trust and confidence in my lab work. Additionally, I would like to thank my co-advisor Professor Young Kwon for his accessibility and collaboration. I would like to acknowledge Professor Claudia Luhrs for her commitment to the Materials Science Department and students. She is the glue that holds the department together.

I would like to thank my classmates. It was an honor to work with each of them. In particular I would like to thank 2LT Sam Lowell for his assistance with data analysis: without his help I would not have been able to accurately interpret all my data.

Finally, I would like to thank my family for their support, patience and love during my time at NPS.

THIS PAGE INTENTIONALLY LEFT BLANK

I. INTRODUCTION

A. SUMMARY OF FINDINGS

This research is a continuation of the study of Super Dielectric Materials (SDM), a class of materials invented at the Naval Postgraduate School (NPS) with dielectric constants, orders of magnitude higher than any previously identified dielectrics [1], [2]. The theory of SDM is that liquid containing dissolved ions will form dipoles in the presence of an electric field. This will create fields that oppose those created by electrons on capacitor electrodes, thereby reducing the net field. Thus, at any given charge on the electrodes, the measured voltage will be significantly less than that observed in the absence of the SDM. Capacitance is defined as, the amount of charge stored as a given voltage. SDMs increase capacitance, as do all dielectrics, but will do so to an unprecedented extent. This theory is a modification of the classic theory of dielectric materials, the so-called ponderable media model [3].

The first SDMs tested were composed of a particularly high surface area refractory alumina oxide powder, herein referred to as three micron alumina, filled to the point of incipient wetness (paste consistency) with aqueous solutions of either boric acid or sodium chloride [4], [5]. The average pore size in the alumina powder used in the earlier work was on the order of 250 Å in radius. Hence, once filled with aqueous salt solutions, ionic charge separation resulting from the applied field could create dipoles on the order of 500 Å in length; far greater than the separation in the best solid dielectrics(barium titanate) which is approximately 0.1 Å in maximum length [2]. This increase in dipole length, combined with high salt concentrations, was postulated to explain the increase in low frequency observed dielectric values, about five orders of magnitude ($\sim 10^9$) greater than the best reported dielectric materials.

The initial work [1] with one type of SDM left many questions. First, is the theory of SDM truly universal? Will the effect be observed in all types of salt solution filled, porous, electrically insulating, refractory oxides? Are the dielectric constants

different for different media, in particular, can even higher dielectric constants be obtained? Does the salt employed impact the measured dielectric constant?

The results of the present work show clearly that the SDM model, as postulated, applies to a large family of materials. This family clearly encompasses many electrically insulating, porous refractory oxides filled with many salt solutions. Specifically, SDM behavior was observed using two high surface area forms of alumina, a high surface area silica and fumed silica. Moreover; two different salt solutions were employed in each of these materials, and SDM behavior was observed in all cases. The study found that the dielectric constant was a strong function of the refractory oxide employed. Values of dielectric constants varied from a low of $3x10^{9}$ to a high of $7x10^{11}$. A more thorough search may reveal members of the powder-SDM class with even higher dielectric constants, hence even higher energy densities.

In addition to the primary results listed above, the research suggested some unfortunate limits to SDM based capacitors. For example, as shown before, the maximum operational voltage is about 1.0 V. Also, the internal resistance is on the order of 100 kΩ, hence SDM, like other capacitors, will hold a charge on the order of hours, not days.

B. MOTIVATION

As the military moves toward a digital battlefield, the need for inexpensive and reliable portable power sources is an obstacle that must be overcome to provide soldiers and sailors full electronic capability without hindrance due to size, weight or operating costs [6]. The next generation of weapons, such as rail guns and high-powered lasers, requires a dramatic increase in electrical power over current conventional weapon systems [7]. All of this must be accomplished in the worst operating conditions, to include urban warfare and adverse weather conditions, all while supporting forces with simple logistics.

The military is looking for a battery/capacitor system to fill the gap for portable electric power. Batteries are part of society's everyday life, from smart phones to laptop

computers. The U.S. military uses batteries to power radios, unmanned aerial vehicles (UAVs), medical devices, computers, and power supply circuits.

The need for capacitors in conjunction with batteries to form long-lasting portable "energy systems" is not a new idea. The basic explanation is capacitors can buffer batteries against power surges, which significantly decreases the life of "unbuffered" batteries. This is accomplished by using batteries to slowly energize capacitor banks, then use energy stored in the capacitor to provide bursts of high power. However, current capacitors are significantly less energy dense than top-rated batteries [8]. The best supercapacitors have approximately one percent of the energy density of lithium ion batteries. This means using the current generation of capacitors to better manage power surges increases the size and weight of a battery system, which poses a major impediment in some applications. For example, the Air Force Space Program requires electric thrusters to maintain a satellite's station [9]. Sudden "bursts" of battery power are required to fire jets that reposition a satellite. These "bursts" significantly degrade the battery's life; however, there is no additional space on a satellite to accommodate a bulky capacitor bank [10]. Similar degradation is experienced with hand-held radios in the field due to the peak power required when keying a radio. Integrating capacitors into this system increases the life of the battery, and consequentially the system [11]. Unfortunately, as previously noted, bulky capacitors cannot be accommodated by individual service members, thereby necessitating smaller and lighter battery/capacitor systems in the field.

The importance of reducing capacitor size by increasing the energy density is even more critical for weapons designed for an "all electric Navy." For example, the Navy is currently testing the Laser Weapon System (LaWS) on *USS Ponce* (LPD-15). The LaWS requires megawatts (MW) of power to damage/destroy a target with a surface area of approximately 100 cm^2 [12]. A battery cannot generative the power required. Batteries derive energy from a chemical process that involves ionic diffusion, meaning by nature they cannot deliver enormous amounts of power in milliseconds. Conversely, capacitors work by directly releasing pre-energized electrons from storage on a

conductive electrode, providing immediate and efficient power [13]. Figure 1 shows the energy, power and time tradeoffs between capacitors and batteries.

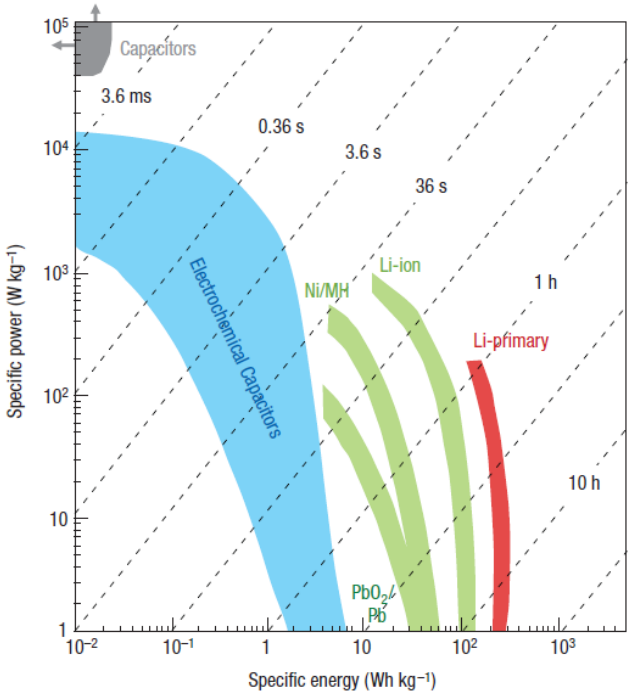

Figure 1. Specific power vs. Specific energy of electric storage devices, from [14]

The greatest problem faced by current capacitors is size. The space needed for a capacitor bank to fire a new weapon system does not fit the compact requirements of any naval vessel or satellite. Supercapacitors also known as electric double layer capacitors (EDLC) or ultracapcitors, are the best energy storage capacitor (35 J/cm^3) in use [15]. Commercial batteries average 200 J/cm^3 [16] and the newest lithium-ion batteries have a volumetric energy density between 250 to 620 Wh/L (900 to 2230 J/cm^3) [17]. This simply means the best prototype supercapacitors have an energy density one tenth that of the best lithium ion batteries. Table 1 lists the tradeoffs between a lithium ion battery and electrochemical capacitor (supercapacitor).

Table 1. Comparison of electrochemical capacitors and lithium-ion batteries, from [8].

Characteristic	State of the Art Lithium Ion Battery	Electrochemical Capacitor
*Charge time	~3–5 minutes	~1 second
*Discharge Time	~3–5 minutes	~1 second
Cycle life	<5,000 @ 1C rate	>500,000
Specific Energy (Wh/kg)	70–100	5
Specific power (kW/kg)	**0.5 -1	5–10
Cycle efficiency (%)	<50% to >90%	<75 to >95%
Cost/Wh	$1–2/Wh	$10–20/Wh
Cost/kW	$75–150/kW	$25–50/kW

** Time for discharge and charge of the useable total energy stored in the devices.*
*** Power capability of the battery for short duration partial discharge at 90% efficiency.*

In order to achieve the energy densities required to power new weapon systems, a shift in capacitor technology is required. Today's commercial supercapacitors have inadequate energy density and are cost prohibitive. To improve these shortcomings, research is focused on increasing the specific surface area. The ultimate energy density of a theoretical graphene based supercapacitor is still too low and the projected price is prohibitive. Therefore, a new type of capacitor must be developed, one that is not based on the increased specific surface concept of supercapacitors.

1. Capacitor Technology

Capacitance is defined as a body's ability to store an electrical charge. All objects have capacitance which is defined as the amount of charge an object can hold at a given voltage. Equation (1) is the basic equation for capacitance where Q is the charge given to one plate and V is the potential difference of volts [18].

$$C = \frac{Q}{V} = \frac{\text{Charge}}{\text{Potential Difference}} \tag{1}$$

Electrostatic energy is stored in a capacitor when a voltage is applied to an insulating medium separated by two conducting surfaces [19]. Energy is released when

the circuit is short-circuited. Several factors influence the capacitance of an object. The shape of a capacitor is just one example. The capacitance of a charged sphere with two concentric spheres is given in Equation (2) and shown in Figure 2, here ε_R is permittivity of free space, ε_0 is dielectric constant, and a and b are the radii of the sphere.

$$C = 4\pi\varepsilon_0\varepsilon_r \frac{ab}{b-a} \tag{2}$$

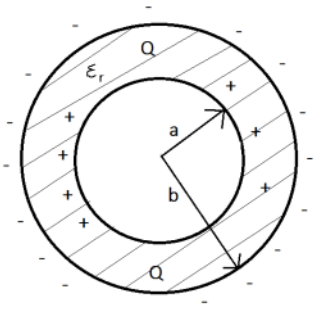

Figure 2. Spherical capacitor

In contrast, parallel plate capacitors (Figure 3) use Equation (3) for capacitance. Two plates with an area of the electrodes *A* are separated by a thickness of *d*.

$$C = \varepsilon_0\varepsilon_R \frac{A}{d} \tag{3}$$

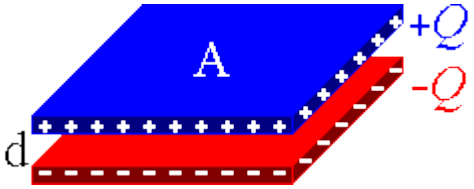

Figure 3. Parallel plate capacitor, from [20]

The main difference between these shapes is distance (*d*), and its effect on capacitance. Increasing the capacitance of a spherical capacitor requires an increase in total size. Conversely, decreasing the thickness of a parallel plate capacitor concomitantly decreases the total size and increases capacitance. Consequently, for a parallel plate

capacitor, decreasing the size decreases thickness, which is why all commercial capacitors use some form of parallel plate capacitors.

Examining types of capacitors helps to understand all other factors that determine the amount of charge that an object can hold at a given voltage. Today's commercially employed capacitors are as follows: electric double layer, electrolytic and electrostatic capacitors. Examples are shown in Figure 4. In a broad sense, all of these capacitors are considered parallel plate geometry, meaning they consist of two electrically conductive plates (electrodes) with some form of non-conductive dielectric material between the plates. Using this concept of geometry, it is obvious that capacitance increases as size decreases. The ultimate objective of capacitors for energy storage applications is to increase capacitance and maximize energy density.

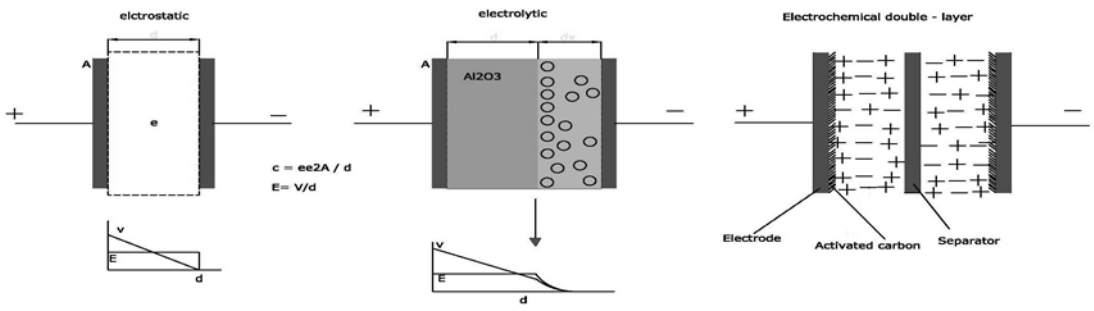

Figure 4. Diagram of different capacitor configurations, from [21]

All of these capacitors use a non-conductive material to serve as the dielectric material. Each dielectric has different characteristics, which dictate its ability to store energy under an electric field. This characteristic is known as the dielectric constant (ε_0). Research on new types of capacitors also uses capacitance of parallel plate electrode with dielectric separator with respect to Equation (3). The equation contains three physical variables: area of electrodes (A), distance between plates (t), and dielectric constant (ε_0). All three of these variables have the potential to increase capacitance. All capacitor research is based on improving one of these three parameters (A, t, or ε_0) as discussed below.

a. Electrical Double-Layer Capacitor-Increase Area (A)

Today's most researched form of capacitor is the electrical double-layer capacitor (EDLC) also known as a supercapacitor. EDLC research focuses on increasing the electrodes surface area, *A* in Equation (3). This is accomplished by using a high surface area electrically conductive carbon at a single potential in contact with an electrolyte (typically ionic liquid) at another potential [22]. The charge must be kept below the discharge voltage (e.g., ~1.3 V for aqueous electrolyte) to ensure charge does not flow between carbon and electrolyte. This is because water has a narrow electrochemical stability window [22]. Other solutions with a higher decomposition potential of electrolyte (3-5 V) are doubtful due to safety, technical, and cost constraints [23]. Rather than flow, charge is captured in the electric double layer that consists of carbon on one side and a layer of polarized molecules in the electrolyte. This mechanism of charge along with the layers gives rise to the name electrical double-layer capacitor.

The EDLC structure follows Equation (3) where the surface area of the carbon, an electrically conductive material, is the electrode area (A). The double layer combines both the dielectric constant of double layer and thickness, meaning these two terms are not considered separately in EDLC. The increased capacitance is due to a combination of the following: (i) a very small distance separates the opposite charges in the electrical double-layer; (ii) highly porous electrodes create an extremely high surface area thus increasing the amount of charge stored [24]. There are no simple and reliable methods to measure the thickness of the double layer, nor to directly measure dielectric constant. Thus these parameters are "bundled" in the EDLC literature and for engineering analysis a bundled parameter "capacitance per unit surface area of carbon" is employed, which has a value of approximately 10–16μF/cm^2 of carbon [24].

Many recent studies are focused on using graphene as the carbon electrode in the next generation of EDLC because graphene is the electrically conductive material with the highest known surface area (2,630 m^2/g) [22]. It also has the highest electron mobility of any electrically conductive material [22]. Current published data for commercially available EDLCs have an energy density between 10–90 J/cm^3 [25]. Calculations performed on Maxwell Ultracapacitors were at best less than 35 J/cm^3 [15]. The best

prototypes have an energy density around 300 J/cm^3 (Table 2). Despite the increase in capacitance, EDLC development is still limited to surface area, ultimately limiting the energy volume.

Table 2. Recent advances in high energy storage capacitors. TSDM are in par with EDLC and far above ceramic capacitors, after [5]

Electrical Double Layer Capacitors						
Electrodes	**Electrolyte**	**F/g**	**F/cm^3**	**J/g**	**J/cm^3**	**Ref.**
Activated Carbon (AC)	Aqueous	238	119[a]	86.4	43.2[a]	[26]
Compressed Activated microwave Expanded Graphite Oxide	Ionic Liquid	147	110	227	173	[27]
Activated Carbon	Deep Eutectic	140	70[a]	260	130[a]	[28]
Graphene	Ionic Liquid			306	153[a]	[29]
Carbon nanotubes on Carbon nanofibers	Ionic Liquid			356	178[a]	[30]
Graphene	Organic	298	212	457	324	[31]
Ceramic, electrostatic capacitors						
Dielectric Material		**F/g[1]**	**F/cm^3**	**J/g**	**J/cm^3**	**Ref.**
Aqueous solution of sodium nitrate in titania nanotubes		34	114	70	230	[32]
Polymer					27	[26]
Lead lanthanum zirconate titanate					22	[33]
Barium titanate nanocubes					5	[34]

[a] Volumetric values are estimated assuming a bulk density of 0.5 g cm^3 for carbonaceous electrodes [30].

Note: All values of energy density are either taken from the original paper or calculated using the highest operational voltage shown therein.

b. Multi-layer Ceramic Capacitor-Decrease Thickness (d)

The second approach to increase capacitance studies the multi-layer ceramic capacitor (MLCC) which consists of hundreds of alternating layers of electrode and dielectric ceramics [21]. This approach decreases the thickness of the capacitor by decreasing the distance between flat metal plates, which minimizes the dielectric thickness; see d in Equation (3). At present, each layer in an MLCC has an approximate thickness of 0.5 microns, and despite this remarkably low thickness they have a net energy density less than 10 J/cm^3 [35].

There are three limitations associated with the MLCC. First discharge voltage is a function of thickness, which is a concern when using a micron scale [36]. Second, MLCC use some derivative of barium titanate, which results in a lower dielectric constant due to the presence of fine strains, mechanical stresses, interfacial layers or rough interfaces [37]. Third, the dielectric reaches the saturation level, which prevents a higher energy density [36].

The third limitation listed above focuses on the following fundamental theory of physics: A dielectric material reacts to an applied field by becoming polarized; positive charges are displaced in the direction of the field while negative charges are in the opposite direction shown in Figure 5 [38]. This process leads to a reduction of the net field and voltage across the electrodes. Using barium titanate as a dielectric material causes the charge/voltage ratio to increase, typically by an order of 1000X. As a result, the charge required to produce a specific net field/voltage is thousands of times greater when using barium titante as a dielectric.

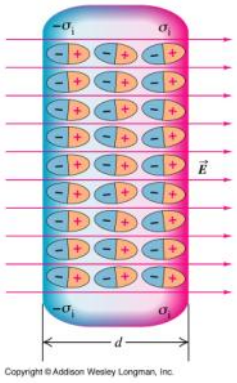

Figure 5. Polarization of dielectric material, from [39]

Voltage from the charge/voltage ratio is limited by saturation however. Net capacitance is constant as long as the strength of the dielectric dipoles increases linearly with the field. This is a concern since barium titante and similarly polarizable media have a maximum dipole length and density [2]. Once this length is reached, saturation occurs and any additional increases in the applied field do not increase the dielectric production in the field. As a result, there is a near linear capacitance reduction above the saturation voltage. Therefore, saturation voltage is a function of thickness and follows the parallel plate rule where the applied electric field (E) is a function of voltage (V) over thickness (d) as listed in Equation (4). It is clear that the applied electric field is inversely proportional to the distance between electrodes. When working with a thin capacitor, on the order of one micron, the saturation field is reached at low voltages, ca. 1 volt. Meaning, the saturation effect limits the thinnest of a capacitor and ultimately the energy density.

$$E = \frac{V}{d} \tag{4}$$

c. Super Dielectric Material-Increase Dielectric Constant (ε_0)

The final parameter used to increase energy density is the dielectric constant. For decades it was generally believed that increases in dielectric constant beyond those of barium titanate and similar crystal structures were unlikely. As a result little progress was

made. The invention of a completely novel type of dielectric, super dielectric materials by a team at the Naval Postgraduate School (NPS) broke that paradigm.

Standard dielectric materials increase the amount of electric charge stored on a capacitor by lowering the voltage associated with the number of charges. This results from the formation of dipoles in the dielectric that opposes the applied field, thus reducing the net field for any specific charge concentration on the electrode [40]. As capacitance is charge/voltage, the lowering of the voltage for any given number of charges increases capacitance. In barium titanate these dipoles are a fraction of an angstrom (Å) in length meaning longer dipoles would reduce the net field to an even greater extent.

Using this concept, the following hypothesis was formed: a porous (e.g., 500 Å pores), electrically insulating powder (e.g., alumina), filled to the point of incipient wetness (paste consistency) with liquid (e.g., water) containing dissolved salts (e.g., NaCl) will have much larger dipoles than found in any solid, hence will have better dielectrics than any solid [4]. This is accomplished through the use of SDM, a multi-material mixture comprised of ion containing liquids combined with highly porous, electrically insulating powders. The NPS team studied various realizations of this concept and published several studies demonstrating that observation is consistent with this hypothesis. Prior to present work, several systems produced dielectric constants of SDMs greater than 10^{10}, or about six orders of magnitude higher than that of any known solid.

C. PRECEDING INVESTIGATION OF SUPER DIELECTRIC MATERIALS

Work in this field first began when Phillips and Scanlan [5] suggested that micron scale metal particles, electrically insulated with an oxide layer, would have superdielectric values. They hypothesized that the metal itself would have near infinite permittivity, but the oxide layer would prevent conductive metal particles. The focus of this work increased both the dielectric constant and energy density. When measuring the capacitance, they found basic meters, including impedance spectroscopy were designed to measure capacitance at zero ±15 mV and work well for determining capacitance in circuit application. However, for energy storage application zero volts measurements are

useless. Therefore, they employed the RC circuit measurements. Initial data from this hypothesis is listed in Table 3.

Table 3. Super Dielectric Material Capacitors from preceding investigation, from [5]

Sample	Material /treat	Measured C (thickness)	Dielectric Constant	Measured R /normalized R (1 cm)
1	Barium Titanate Powder	1.01 nF (1.9 mm)	50	600KΩ
2	Barium Titinate, sintered pellet [1]	10 nF	500	Not available
3	Teflon	16 pF (10 mm)	2.3	>10 MΩ
4	Ni/34cc*	15.0 μF	1,200,000^	N/A
5	Ni/34cc*	15.2 μF (3mm)	650,000	65K/215 KΩ
6	Cu/15cc*	0.33μF (1.6mm)	50,000	2K/13KΩ
7	Fe / 34 cc; Double bake**	2.61 μF (1.6 mm)	60,000	6.3K/41KΩ
8	Zn/TEOS	7.2 μF (1.8mm)	84,000	9.5 K/136KΩ
9	Cr/34ccDouble bake	0.10 μF (1.8 mm)	3,000	20 K/277 KΩ
10	Ni/TEOS	65 μF (1.8mm)	~3,200,000	2.7 KΩ/18 KΩ
11	Zn/TEOS	0.6 μF (1.8mm)	18,020	9.0 K/129KΩ
12	VX-72 TEOS	>500 μF (1.6mm)	$>10^6$	1.1K/18 KΩ
13	'Puck' Ni-TEOS/ Wax	>500 μF	$>10^6$	
14	'Puck' V7H TEOS/wax	0.8 μF	55,000	24K/150 KΩ

TABLE I: TABLE I: Reliable MMD Data, from measurement or literature. Simple tests with standard Agilent capacitance meter yield values consistent with those anticipated for well known dielectrics (Samples 1-3). Remarkably, samples made from MMD materials produced unprecedented dielectric constants (Samples 4-9). Indeed, Barium titanate (Sample 3) is generally considered 'best'. Some values independently verified at Los Alamos National Lab. 'Pucks' made with MMD particles sealed in wax (see Text) were further tested for time constant directly by measuring discharge through a known resistance.

[1] Derived from dimensional values provided in recommended literature.
* 20 gms of metal (all metals Sigma Aldrich, reported better than >98% purity, and mean size 5-10 μ) powder, slowly mixed with noted number of cc of 20% hydrogen peroxide, then baked in air at 100 C for approximately 10 hours.
** Same procedure as *, but done in two steps, each step using half the hydrogen peroxide listed.
^ Independent measurement by Los Alamos National Lab team.

LT Samuel Fromille [1] examined SDM characteristics by creating a composite electrolyte dielectric (CED). This was accomplished by adding micron-scale nickel powder treated with H_2O_2 to electrolyte material which formed an electrostatic capacitor dielectric. The dielectric constant with respect to ratio of metal particles was studied

along with capacitor thickness, resistance, and applied voltage. He successfully proved the SDM theory and repeatedly achieved dielectric constants to the order of 10^{10} operating at an operating voltage greater than 1 V [1]. He achieved dielectric constants that were six orders of magnitude higher than any previously measured. This study revealed SDMs retained high relative permittivity, even with loading fractions in excess of percolation threshold. The limiting operating voltage due to electrolysis of water and complex loss behavior hindered this capacitors design.

D. PRESENT OBJECTIVE

This study focused on systematically testing materials that fit the description of powder based SDMs; porous electrically insulating powder, filled to the point of incipient wetness (paste consistency) with liquid (e.g., water) containing dissolved salts (e.g., NaCl). In earlier work, only a few randomly selected, porous powders and salt solutions were tested. These combinations of insulating powders and dissolved salt solutions were not optimal. The following question is addressed in this study: If the dielectric constants of these randomly selected systems were already ~10^{10}, can higher values, ca. (10^{13}) be achieved with optimal systems? To this end, in the present work the dielectric constant of materials composed of four different porous solids (silica, fumed silica, moderate surface area alumina and high surface area alumina) and two different aqueous salt solutions (sodium chloride and ammonium chloride) were systematically studied and dielectric constants ranging from 10^{9} to 10^{11} were measured.

II. EXPERIMENTAL METHODS

A. EXPERIMENTAL SETUP

In order to better understand the behavior of the SDM capacitor as an energy storage device, charge and discharge rates must be studied. Thus this study focused on determining the capacitance and hence the dielectric constant. The objective was to determine the energy storage potential of the capacitor, rather than high frequency behavior appropriate for electronic applications such as filtering.

All means of measuring capacitance, such as cyclic voltammetry (I=*f*(E), galvanostatic charge/discharge (constant *I*), external resistor discharge (constant *R*) and impedance spectroscopy have limitations [23]. Thus, it is important to select the method that provides data appropriate for the proposed application. For example, "impedance spectroscopy," the method associated with hand held multi-meters and far more sophisticated devices, is based on deconvolution of RC time constant data collected at a single voltage, in general 0 ± 15 mV. In the more sophisticated devices, the impedance as a function of frequency can be deconvoluted from the data. However, in no case is the energy output during the discharge part of the cycle ever directly measured. It can only be inferred from a model of capacitance and some additional data regarding the maximum voltage that can be achieved. This is not an adequate means to measure the actual energy released by a fully charged capacitor during discharge.

In this research, capacitance was measured using the classic RC time constant method. This is also the case for other modern studies of dielectric materials used in energy storage capacitors. This was accomplished by first charging the SDM capacitor with a constant voltage source. Then the capacitor was discharged by placing it in parallel with a voltmeter and known resistor. Figure 6 depicts the capacitor charging in a standard resistor/capacitor (RC) discharge circuit.

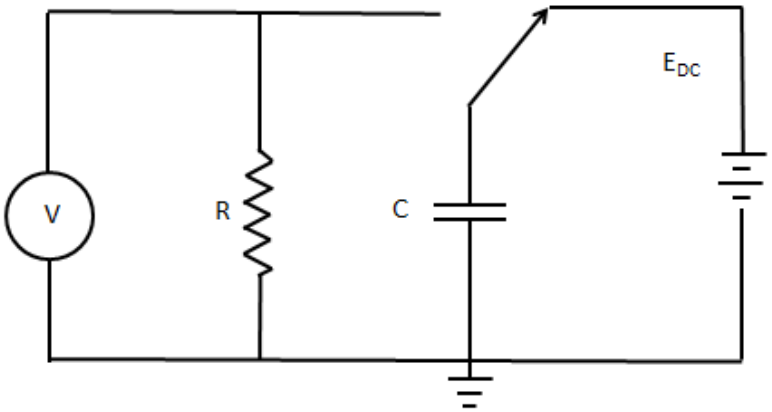

Figure 6. Circuit to measure capacitance, from [1]

The capacitor is charged for a specified period and then switched to discharge through the resistor. The voltage drop across the circuit is measured by the voltmeter and timed. The drop in voltage across the RC circuit is calculated using Equation (5),

$$V(t) = V_o e^{\frac{-t}{RC}}, \tag{5}$$

where *V(t)* is the voltage at a given time, *Vo* is the initial voltage, *t* represents time to discharge, *R* known resistance, and *C* is the unknown capacitance. Plotting $ln(V/V_o)$ vs. *t* produces the slope (*-1/RC*). Then using capacitor geometry and known resistance, the dielectric constant is calculated using Equation (3). Figure 7 is an example of a discharge profile for a 0.22 F commercial supercapacitor.

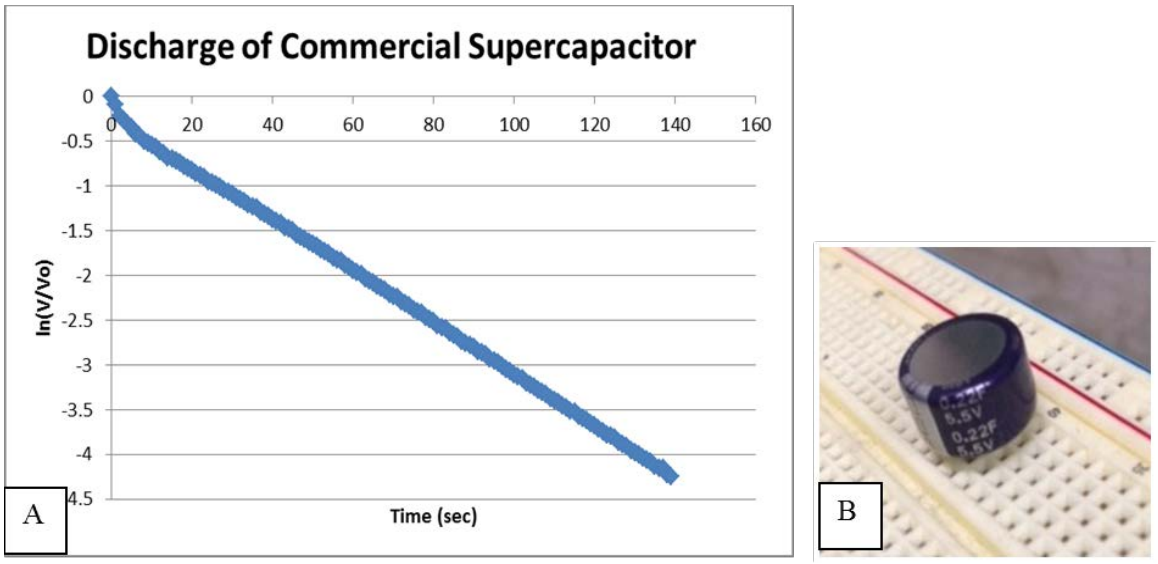

Figure 7. A) Commercial supercapacitor discharge (0.22F)
B) Commercial supercapacitor tested

The same constant slope profile was displayed by the SDM capacitors depicted in Figure 8. A flatter slope represents a slower discharge which translates into a larger capacitance and dielectric constant.

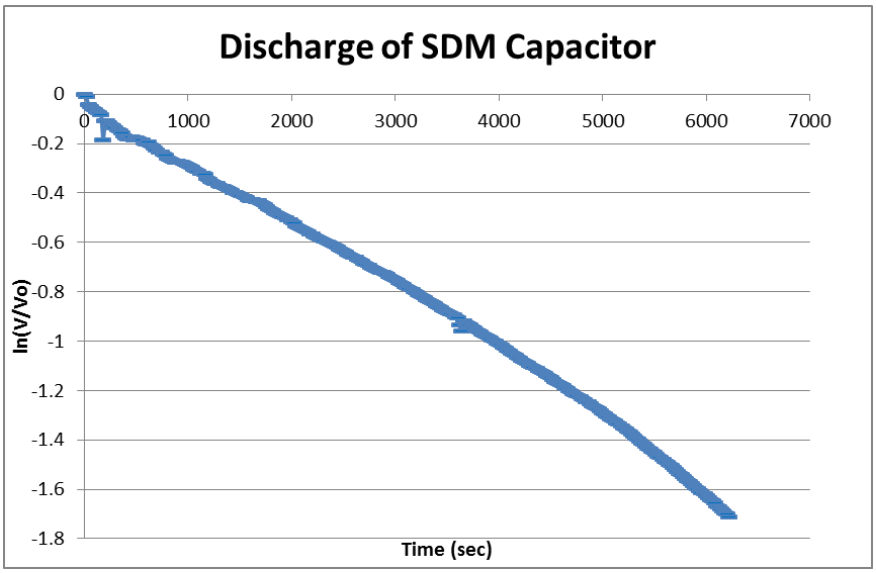

Figure 8. SDM capacitor

In order to validate the continuous charge and discharge cycles, the RC circuit in Figure 6 was modified to allow for monitoring of both the charge and discharge profiles. The new circuit is shown in in Figure 9, where the capacitor and resistor are now in series.

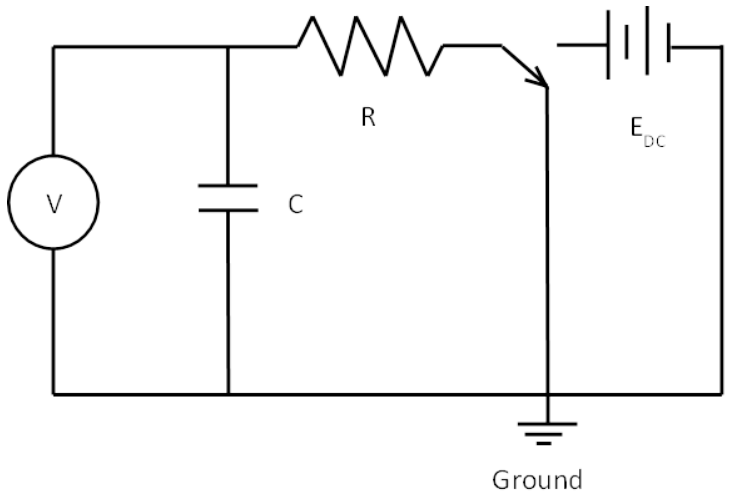

Figure 9. RC circuit monitor charge and discharge, from [1]

B. EXPERIMENTAL PROCESS

The process used in this research was similar to work conducted my LCDR Samuel Fromille in 2013. His technique was modified to meet new objectives. Materials used in this study focused on electrolytes and highly porous insulating materials. Electrolytes employed included sodium chloride and ammonium chloride. Highly porous insulating materials consisted of aluminum oxide (Alfa Aesar, γ-phase, 99.97%, 3 micron APS Powder, S.A. 80–120 m^2/g, CAS # 1344–28–1), silicon dioxide (Sigma-Aldrich 99%, 0.5–10 μm), fumed silica (Aldrich powder, 0.007 μm), and aluminum oxide (Alfa Aesar, catalyst support, high surface area, 1 kg, 1/8″ pellets). The resistor/capacitor setup is shown in Figure 10. Capacitors were charged and discharged using Keithley 2200–20–5 Programmable Power Supply, which provided either four or six volts. The Agilent U1252A multimeter measured voltage across the capacitor. All data was logged using GUI Data Logger.

Figure 10. Setup to measure voltage across capacitor

A custom jig consisting of two aluminum electrodes measuring 1.96 inches (4.98 cm) in diameter were placed in a plastic cylindrical basin. The basin measured 1.98 inches (5.03 cm) in diameter. Figure 11 demonstrates the electrodes and jig setup. A large bucket was placed over the jig to maintain the moisture of the capacitor.

Figure 11. Capacitor jig setup

A Large roll of GTA-grade Grafoil was used to make disks which were cut into circles measuring 0.77 inches in (5 cm) diameter. Circles were cut using a die template and hammer. Figure 12 demonstrates the Grafoil Disks. An additional 5 mm of Grafoil was trimmed from the disk. This was done to ensure the disk was smaller than the aluminum electrodes and prevented spillage due to the weight of the electrodes. Grafoil is made by pressing graphite flakes into thin sheet, it has an average surface area of 22 m^2/g [41]–[42]. The average Grafoil thickness was 0.41 mm. The disks were used as a podium for the dielectric material to be spread. Once the material was evenly spread another Grafoil disk was placed on top. The final product has the appearance of an "Oreo." The Oreo was placed between two Grafoil disks that were not trimmed down. This method ensured even electrode contact against the Grafoil disks.

Figure 12. Die and hammer utilized in cutting Grafoil disk

1. High Surface Area (HSS) Dielectric Composition

The HSA dielectric is comprised of a porous powder material and mixed with an aqueous electrolyte. First, distilled water is added to a selected salt. The ratio is typically close to saturation (35% for sodium chloride) [43]. The solution is agitated by hand to dissolve the salt. Then the high surface area medium is added and mixed together with a spatula to form a paste. The mass of the medium is determined by the material properties, for example fumed silica required more mass than aluminum oxide. More medium or

distilled water can be added on a case by case basis to ensure proper consistency; it must be spreadable and workable as well as firm enough to support aluminum electrodes in the capacitor configuration. Figure 13 demonstrates the mixing and application process.

Figure 13. HSA capacitor assembly process

2. Experiment Design

Experiments were conducted to first examine whether an HSA material had the ability to work as a capacitor by using an electrolyte, either ammonium chloride or sodium chloride. Using the same recipe, a second, thicker capacitor was made. If the capacitor worked, meaning it had three successful charge/discharge cycles; the alternate electrolyte was used to make two capacitors of varying thicknesses. Cycles were measured using the circuit shown in Figure 9 with either 11 kΩ or 20 kΩ. Data was then compared to determine which capacitor had the higher dielectric constant. Further studies doubled the electrolyte concentration.

3. Verification of Capacitor Behavior

After the best combination of high surface area materials and electrolytes were determined, the capacitor was verified by examining the charge and discharge cycles.

Figure 14 shows the difference between the perfect simulated RC models versus the experimental results of an EDLC. Losses are expected, but overall the charge and discharge cycles should resemble the RC model and have smooth lines. Using a 20 kΩ resulted in less noise and smoother plots. Smaller 10 kΩ resistors were used to demonstrate the capacitors ability to quickly deliver power.

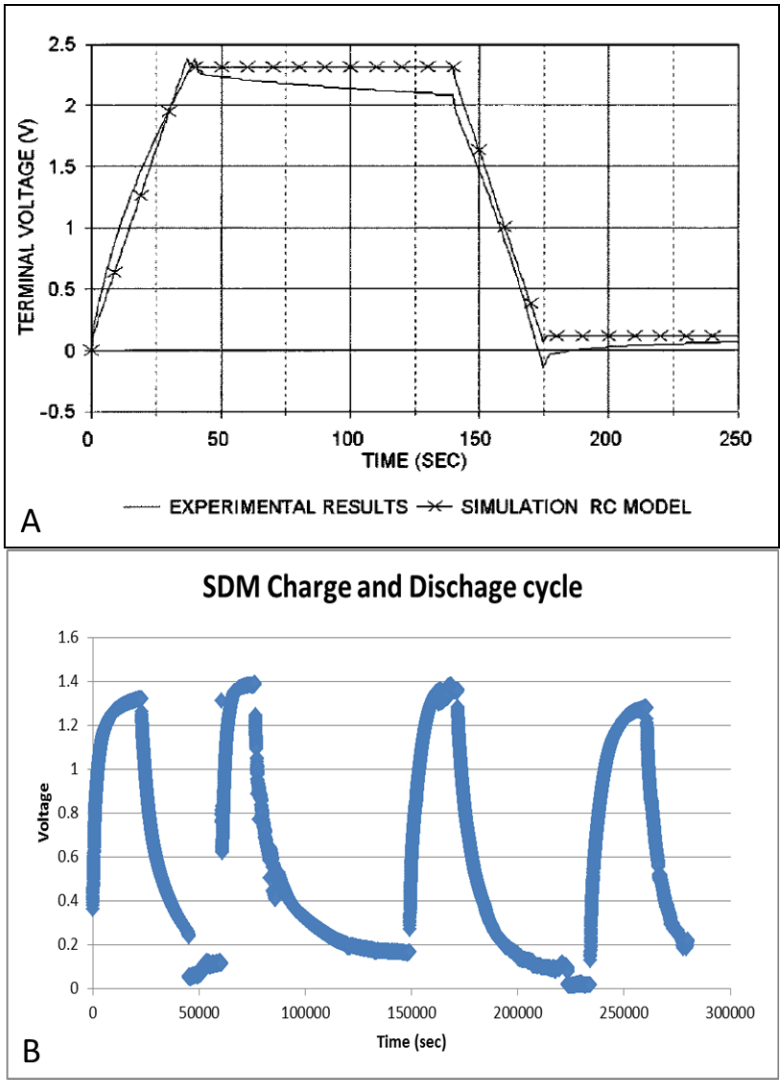

Figure 14. A) Comparison between experimental and RC circuit modeling, from [44], and B) SDM capacitor charge and discharge

III. RESULTS

A. COMPOSITE DIELECTRIC OPTIMIZATION

Combinations for every HSA material and electrolyte were tested. Capacitors were constructed to determine if the following traits affected the dielectric constant: electrolyte concentration, electrolyte, and HSA material. Using this data, a few broad conclusions were reached. First, many porous non-conductive materials (matrix) filled to incipient wetness with solutions (electrolytes), will act as SDM; that is, materials with dielectric constant greater than 10^5, at low frequency (ca. <1Hz). Second, many different soluble salt solutions can be used. Together, these first two outcomes demonstrate that SDM are a large family of materials. Third, the identity of the salt employed to make the aqueous alt solution does not dramatically impact performance. Finally, it is tentatively concluded that fumed silica outperforms other SDM matrix materials probably due to its absorption of salt/water relative to weight and volume.

1. Electrolyte Concentration

This analysis was designed to determine whether electrolyte concentration affects the dielectric constant for one type of matrix material, fumed silica. This series of tests used a 20 kΩ resistor and a 4 V applied charge. The amount of sodium chloride in the aqueous salt solution was increased with each new capacitor built, thus increasing the relative saturation level. Also, the ratio of solution to matrix material was held constant. Salt concentrations ranged from 0.2 parts (or 9.1% of saturation) of water to 2.28 parts or approximately 71.3% of known saturation.

The capacitor was charged and discharged a minimum of three times. The data in Table 4 lists the percent of salt used compared to the known saturation of sodium chloride. Data is plotted in Figure 15. The results show the dielectric constant increases, for both computational approaches, as the percentage of electrolyte increases. In the first method, computation was based on determination of capacitance, and subsequently dielectric constant, from a linear fit of $\ln(V/V_0)$ vs time^{-1} over the voltage range ~0.7 to ~0.3 volts. The second approach (in parenthesis, Table IV, column 4) required three

steps: i) use Equation (6) to determine the stored energy by integration of full discharge curves, ii) use the stored energy value in Equation (7) to determine capacitance and iii) from capacitance use Equation (3) to determine the dielectric value. This data also demonstrates that the measured operating voltage increased with the salt loading, potentially leading to much higher energy density. However, the solubility of the electrolyte determines the maximum amount of salt concentration. The solubility of sodium chloride is around 35.7% by weight in water [43].

$$Energy = \sum \frac{V^2 \times \Delta t}{R} \tag{6}$$

$$E = \frac{1}{2} C V^2 \text{ where } V^2 = V_0^2 - V_f^2 \tag{7}$$

Table 4. Electrolyte Level Comparison

Concentration	Composition By Parts	Dielectric Thickness (mm)	Average Dielectric Constant	Operating Voltage (V)	Average Capacitance (F)
7APR14 9.1%	0.2-NaCl 6.6-H2O 1-Fumed Silica	0.31	1.47E9 (2.06E9)	0.94-0.05	0.13
6APR15 28.6%	0.83-NaCl 8.83-H_2O 1 Fumed Silica	2.3	5.82E10 (3.27E10)	1.09-0.09	0.28
13APR15 41.6%	1.33-NaCl 8.83-H_2O 1-Fumed Silica	2.5	1.06E11 (8.5E10)	1.23-0.17	0.58
28AUG15 71.3%	2.28-NaCl 8.92-H_2O 1-Fumed Silica	2.5	1.31E11 (1.24E11)	0.93-.28	0.89

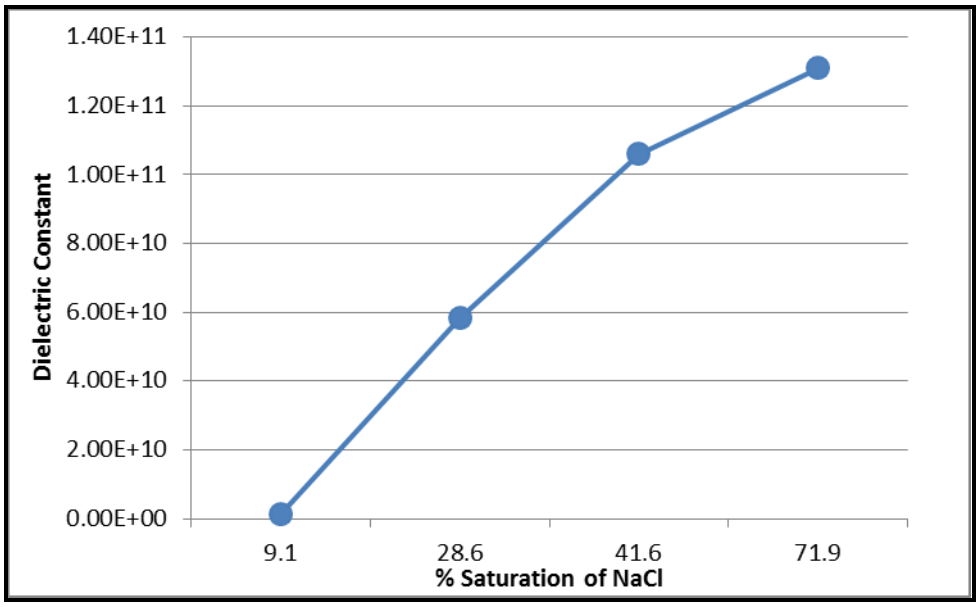

Figure 15. Dielectric constant vs. percent saturation of sodium chloride

Figure 16 compared three of the matrix materials with sodium chloride electrolyte concentrations around 40%. Error bars represent the differences between the highest and lowest values of the three averaged dielectric constants. Fumed silica had the greatest dielectric when comparing the same concentration proposing it as a superior matrix material.

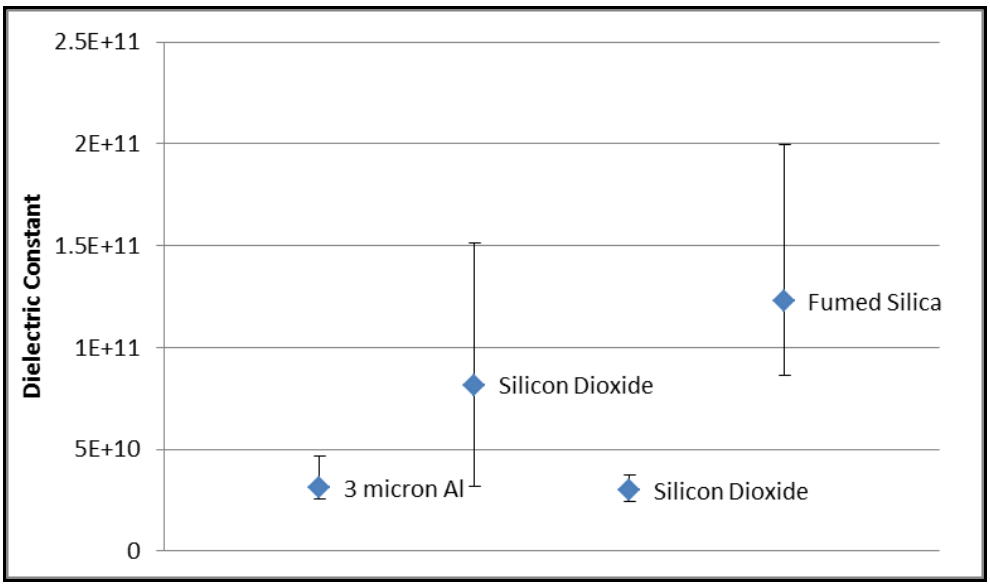

Figure 16. Comparison of ~40% solubility of sodium chloride electrolyte

It is notable that success with the lower salt concentrations had mixed results. Four attempts were made to construct a capacitor using mixtures with ~10% sodium chloride to water. In only one case was any capacitive behavior observed. In the other cases, the disk behaved like a resistor. There was no evidence of increasing voltage drop with charging time and no evidence during discharge that any charge was stored. This ratio proved to be too little salt, resulting in none of the capacitors charging.

One explanation for the one success at ~10% salt related to the age of fumed silica. Fumed silica is known to be extremely hygroscopic, meaning water concentration increases with time, fundamentally modifying the character of the material. In fact, according to the manufacture fumed silica has a shelf life of approximately two years [45]. The successful experiment conducted with just 8% sodium chloride was performed a year prior to the three other attempts. Material properties may have changed over time, which may explain why tests with a smaller salt ratio failed. The percentage of salt may have a larger impact on material grain size and texture.

2. Electrolyte Selection

The second analysis conducted sought to determine which electrolyte solution led to a higher dielectric constant. Capacitors with either sodium chloride or ammonium chloride were constructed with the following high surface area mediums: silicon dioxide, three micron alumina, fumed silica or aluminum oxide pellets. The highest average dielectric constant of each combination was chosen to represent data (Table 5). The results show that there is no clear and consistent difference in dielectric constant as a function of electrolyte. In matrix material, three micron alumina, the aqueous sodium chloride solution yielded a dielectric value almost an entire order of magnitude higher than its counterpart. The large difference seen in three micron alumina and sodium chloride may be a result of using only a 10.8 kΩ resistor compared to a 20 kΩ resistor used other tests. However, the salt identity in all other cases led to only a small difference in performance.

Table 5. Electrolyte material

Sodium Chloride						Ammonium Chloride					
	Composition	Dielectric Thickness (mm)	Dielectric Constant	Operating Voltage (V)	Capacitance (F)		Composition	Dielectric Thickness (mm)	Dielectric Constant	Operating Voltage (V)	Capacitance (F)
04AUG14	0.6g NaCl 2.3g H2O 2.0g 3 Micron Alumina	1.53	3.96E10	0.96-0.15	0.43	28OCT14	0.61g NH_4Cl 4.25g H_2O 0.62g 3 Micron Alumina	0.45	1.18E10	0.94-0.28	0.69
21APR14	0.20g NaCl 1.88g H_2O 1.2g Al_2O_3	0.222	8.82E9	1.25-0.21	0.69	24FEB15	0.13g NH_4Cl 1.50g H_2O 2.51g Al_2O_3	1.71	3.28E10	0.84-0.12	0.33
28Aug15	1.38g NaCl 5.35g H2O 0.61g Fumed Silica	2.5	1.31E11	0.93-0.28	0.89	6JUL14	0.61g NH_4Cl 4.65g H_2O 0.6g Fumed Silica	1.82	7.40E11	0.91-0.17	0.60
02MAR15	0.25g NaCl 1.65g H_2O 3.70g Silicon Dioxide	1.11	4.01E10	0.89-0.30	0.63	23JUL15	0.26g NH_4Cl 1.65g H_2O 4.04g Silicon Dioxide	1.82	2.73E10	0.94-0.15	0.44

Figure 17 compares the average dielectric constant for all combinations of HSA materials and electrolytes where circles represent outliers. With the exception of three micron alumina, all dielectric constants are close in value for each material. This suggests there is no difference between the electrolytes and both are suitable SDM materials.

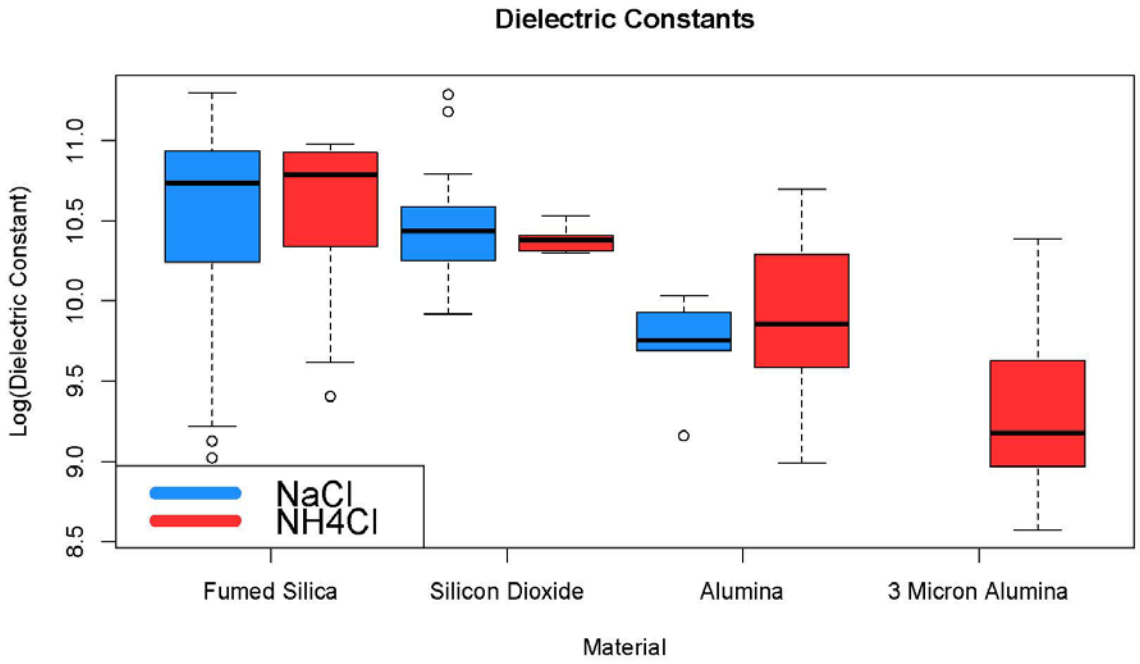

Figure 17. Average dielectric constant values

3. Thickness

This study examined the dielectric constant as a function of thickness. The dielectric constant is a material property and calculated by measuring capacitance using the RC time constant when area, permittivity of free space, and thickness are known and constant. Using the same percent solubility, capacitors with varying thickness were tested. An operating voltage between 0.7–0.3 V was used to determine the dielectric constant. Based on data listed in Table 6, the dielectric constant is not inversely proportion to thickness. Figure 18 suggests an optimal thickness (~2.6 mm) is necessary to achieve the highest dielectric constant.

Due to the manual mixing and application process, SDM capacitors are limited to the minimum thickness. Attempts to make a fumed silica capacitor with a thickness of 0.7 mm failed repeatedly. This confirms that manufacturing techniques limit the minimum size and, eventually, the energy density.

Table 6. Dielectric constant (0.7V–0.3V) with respect to thickness

	Composition	Dielectric Thickness (mm)	Dielectric Constant	Capacitance (F)
01JUN15	0.6g NH_4Cl 4.6g H_2O 0.6g Fumed Silica	1.4	5.27E10	0.67
06JUL15	0.6g NH_4Cl 4.6g H_2O 0.6g Fumed Silica	1.8	9.62E10	0.91
4MAY15	0.6g NH_4Cl 4.6g H2O 0.6g Fumed Silica	2.6	1.75E11 (1.24E11)	1.16 (1.02)
13JUL15	0.8g NH_4Cl 5.3g H_2O 0.6g Fumed Silica	4.5	8.65E10	0.33

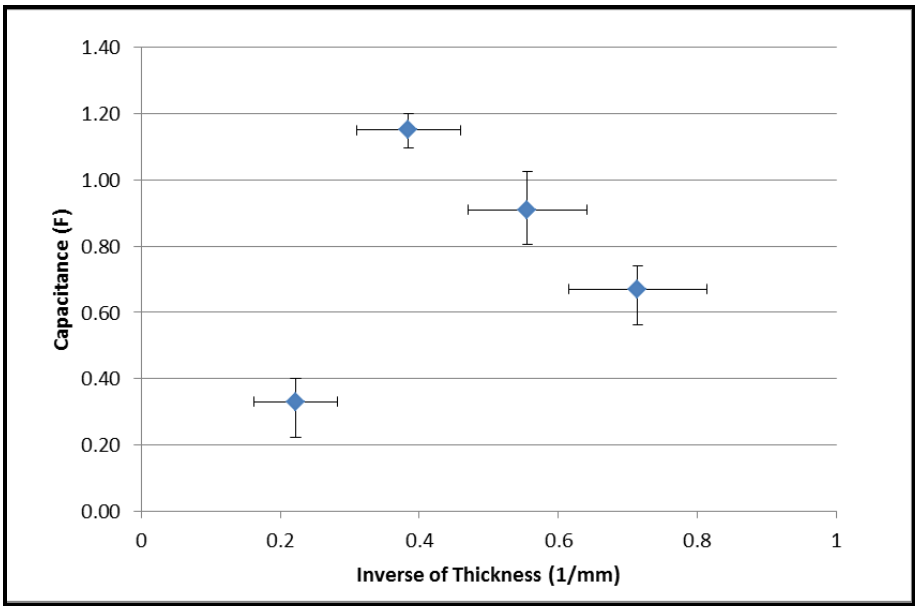

Figure 18. Capacitance vs. thickness relationship

4. High Surface Area Material

High surface area material was selected based on known surface areas of materials not previously tested. The box and whiskers plot (Figure 17) divided data into upper and lower sections and identified the outliers and median. Fumed Silica with ammonium chloride had the highest dielectric. However, fumed silica with ammonium chloride had the largest median dielectric constant. The combination also had the smaller range, suggesting a more consistent capacitor.

Based on Figure 17, silica based HSA material produces higher dielectric constants and electrolytes cause a minimal change in dielectric constant. Additional tests with three micron alumina and sodium chloride using a 20 kΩ resistor are needed to complete dielectric constant sequence.

B. ENERGY DENSITY

A large energy density is highly desired to maximize the use of space and calculated using Equation (8) where C is capacitance, V is operating voltage, and vol is volume of capacitor.

$$\text{Energy Density} = \frac{1}{2}\frac{CV^2}{vol} \tag{8}$$

SDM capacitors have large dielectric constants and capacitance. However, due the size and manual construction, SDM capacitors have a large volume. This combination dramatically reduces energy density to at best 0.17 J/cm^3, significantly smaller than 35 J/cm^3 reported by commercial supercapacitors [15].

THIS PAGE INTENTIONALLY LEFT BLANK

IV. CHARACTERIZATION

A. HSA MATERIAL SIZE

The HSA powder selection was based on known surface areas. In the tentative published SDM theory, matrix material with large pores should create the large dipoles leading to larger dielectric constants. However, the data collected herein is not consistent with this model. The largest dielectric values measured were from materials without significant pore volume or pore size, rather very small particles. That is, fumed silica consistently yielded the highest dielectric values, even though fumed silica has a very high surface area due to the very small size of the particles from which it is composed.

The fumed silica particles with an order of 7 nm, are clearly too small to support internal dipoles of significant length. In contrast, three micron alumina has an average pore size diameter of 350 μm. Even semi-sintered fumed silica particles composed primarily of particles of 7 nm will likely only have pores near the size of the primary particles, hence far smaller than the pores in the three micron alumina. Thus the theory suggests that three micron alumina should have a better dielectric constant than fumed silica. A modification of the model is proposed: In some materials, the dipoles in separate pores are linked to create dipoles of far greater length and charge concentration than possible in a single pore. It is clear from the data with fumed silica that, for the theory to be valid, some linkage must be postulated. Although this modification was inspired by the fumed silica data, it can pertain to all the powder SDM materials. Prior published articles [2] found that the theoretical increase in dielectric constant relative to barium titanate should have been on the order of ~1,000 for porous alumina containing NaCl. However, the measured value was closer to 10^6, greater than barium titanate. The same linkage concept could explain this finding as well.

In order to confirm this general understanding of fumed silica and to properly question the earlier model, the particle size of each HSA material was measured and compared using a Laser Scattering Particle Size Distribution Analyzer and Scanning Electron Microscopy. Only the latter appears to give accurate size information.

1. Laser Scattering Particle Size Distribution Analyzer (LSPSDA)

In Table 7, both the manufacturer's reported surface area and particle size and the size measured using the LSPSDA LA-950V2 are provided. Three separate measurements were taken for each material and averaged. When comparing manufacturer's size to measured particle size, the measured three micron alumina and fumed silica were significantly larger than the size listed on the packaging. This may be a result of agglomeration, or simply result from the inherent limitation of the method. The shelf life of the materials may also affect the particle size. For example, fumed silica has a tendency to absorb moisture; meaning once its packaging is opened agglomeration may occur [45].

Table 7. HSA material particle size comparison

Material	Surface Area (m^2/g)	Known Particle Size (μm)	Measured Particle Size (μm)	Standard Deviation (μm)
3 Micron Alumina	80-120	3	14	50
Ground 1/8" pellets			7	5
Silicon Dioxide	590-690	0.5-10	5	2
Ground Silicon Dioxide			4	2
Fumed Silica	395	0.007	64	40

The large difference between known and measured particle size along with the large standard deviation suggest the LSPSDA is not a valid technique to measure nanoparticles or materials susceptible to agglomeration. The measured size for silicon dioxide was within the known range; however, all other measurements were significantly larger than the reported manufacturer's size. Given the uncertain validity of the laser measurement, a second technique, SEM was employed.

2. Scanning Electron Microscopy (SEM)

SEM images were taken to compare manufacturer reported and NPS measured particle sizes. All HSA powders are nonconductive materials, which required samples to

be placed on carbon conducting tape. Examining nonconductive materials also meant it was difficult to distinguish characteristics. In contrast to the laser method, the particle sizes determined using the SEM were close to those reported by the manufacturer. For example, in the SEM image, it is clear many of the particles in three micron alumina (Figure 19) are 3 μm in size or less. There values are qualitatively close to the reported 3 μm size. No particles appeared to be as large as the 14 μm average obtained from the laser technique

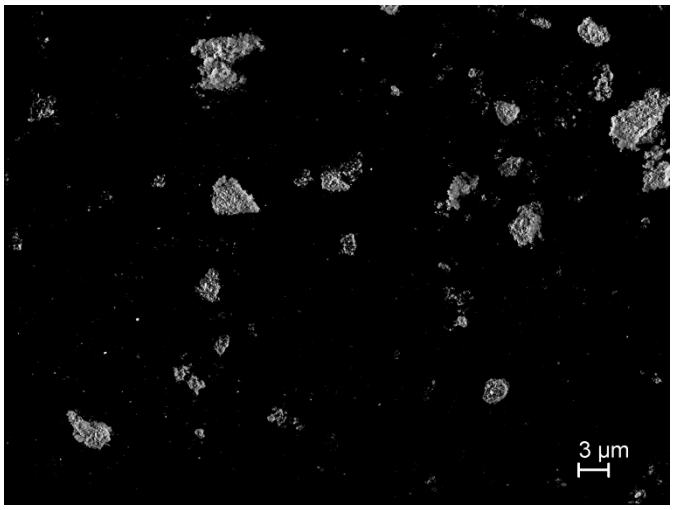

Figure 19. SEM image of three micron alumina (1.1KX)

The aluminum oxide powder used 1/8 inch pellets ground in a blender for one minute. This process resulted in uneven particle sizes, as seen in Figure 20. This may account for a standard deviation greater than the measured particle size as seen by the LSPSDA.

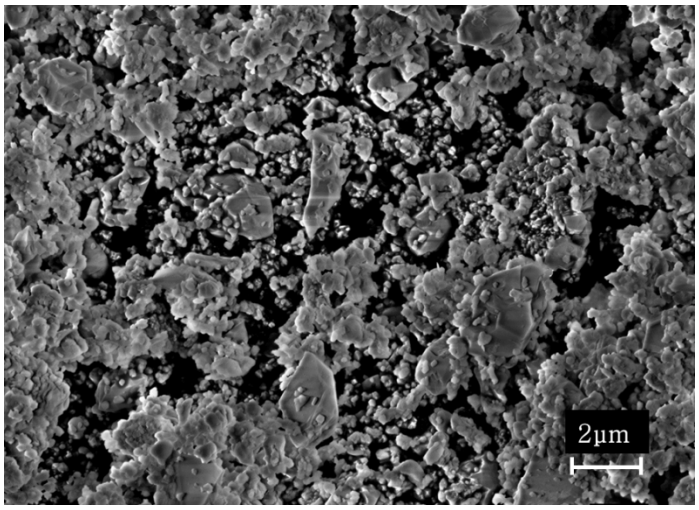

Figure 20. SEM image of aluminum oxide powder (5KX)

Like aluminum oxide, silicon dioxide varies in particle size according to its packaging. Silicon dioxide powder was ground for 10 seconds prior to mixing. This step broke up large clumps of the powder, which assisted in mixing. The SEM image in Figure 21 shows the expected particle size variance and particles smaller than those listed for unground silicon dioxide.

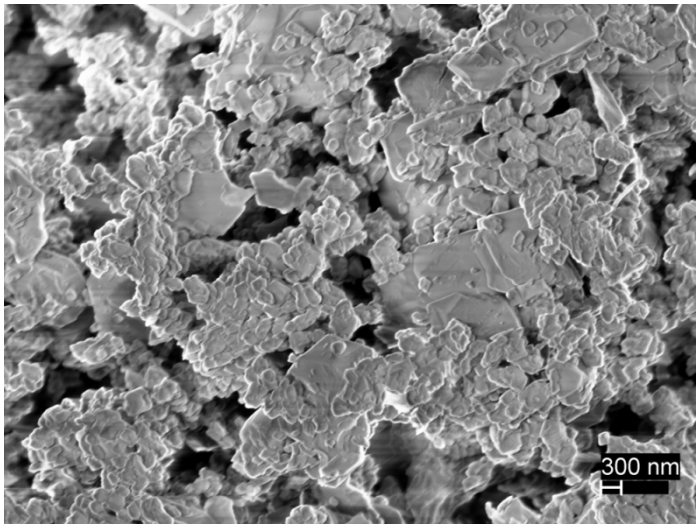

Figure 21. SEM image of ground silicon dioxide (11KX)

Fumed silica has a known particle size of 0.007 µm or 7 nm. Since fumed silica is a nonconductive material, it was difficult to distinguish primary particle sizes on a

nanoscale. The particles observed (Figure 22) are agglomerated from primary fumed silica particles. Increasing magnification resulted in poor images. Overall, particle size measurements on the SEM were the correct order of magnitude and significantly smaller than 64 μm measured using the LSPSDA.

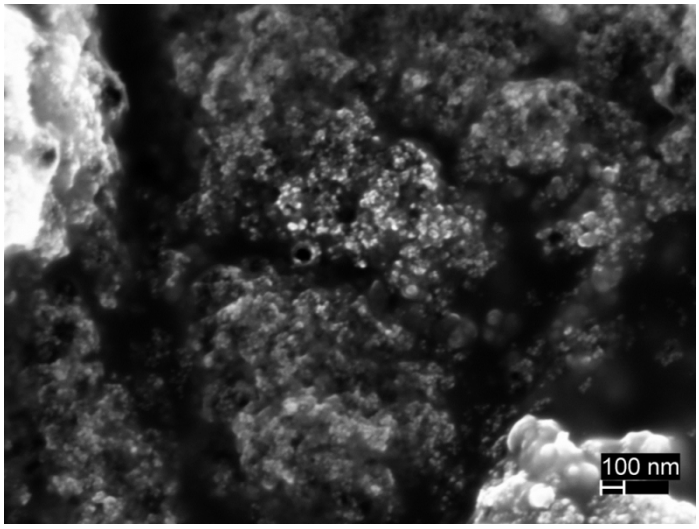

Figure 22. SEM image of fumed silica (37.5KX)

3. Conclusion

Results from the LSPSDA LA-950V2 demonstrated the machine has limited precision when measuring nano size particles. The large standard deviation and complete variance relative to SEM raised concerns about the machines accuracy. One cause for these large values for three micron alumina and fumed silica may be a result of agglomeration and suggests the machine should not be used on powders prone to agglomeration. In contrast, SEM images suggested primary particle sizes close to those claimed in the manufacture provided specifications.

4. Energy Dispersive X-ray Spectroscopy (EDS)

EDS measurements were conducted to determine the chemical composition of each combination. Silicon based HSA material exhibited the expected composition of silicon and oxide (Figure 23). However, according to EDS, aluminum dioxide samples are not mainly comprised of aluminum. Rather, Figure 24 shows they have large amounts

of silicon. There is no data to explain the dominating presence of silicon. Three micron aluminum was mainly comprised of carbon, aluminum and oxide.

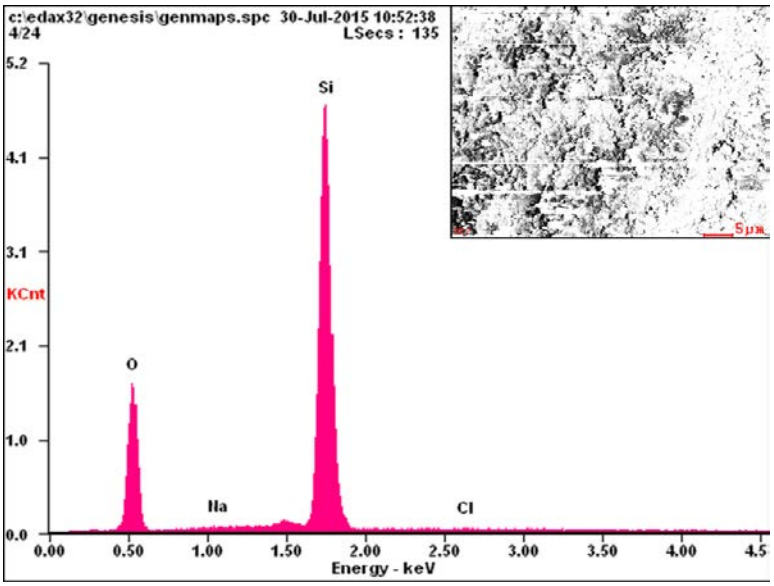

Figure 23. EDS spectrum of fumed silica and ammonium chloride

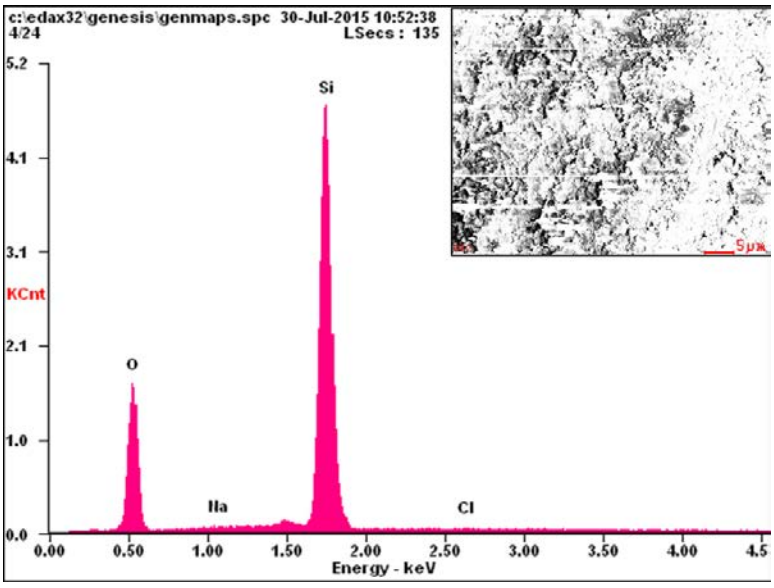

Figure 24. EDS spectrum of aluminum oxide and ammonium chloride

B. INTERNAL AND OUTPUT RESISTANCE MEASUREMENT

An ideal capacitor will charge when connected to a voltage source. Once it is disconnected, it will hold its charge and then discharge without resistance. Instead, all capacitors slowly discharge once they are disconnected from their voltage source. This behavior is known as resistance leakage and can be modeled in an equivalent circuit to result from the presence of a non-infinite internal resistance (R_{int}). The capacitor creates an equivalent circuit with R_{int} parallel and output resistance (R_{out}) in series [46]. The dotted area in Figure 25 represents the theoretical circuit within a SDM capacitor.

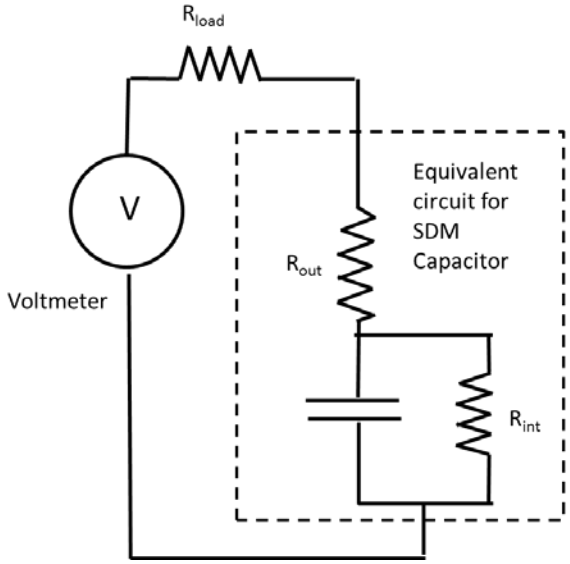

Figure 25. Equivalent circuit for SDM capacitor

When a fully charged capacitor is disconnected from the voltage source and left to sit, the charge will slowly decrease; meaning the capacitor has a leakage resistance or R_{int} resistor. To determine this value, a discharging capacitor is removed from its load, which causes a voltage spike. This behavior is caused by both the load resistor (R_{load}) and output resistor (R_{out}) in the equivalent voltage divider. In Figure 26, a fully charged capacitor discharges for 30 seconds and spikes upon open circuit. V_{load} is the recorded voltage at open circuit and V_{peak} is the recorded voltage after open circuit.

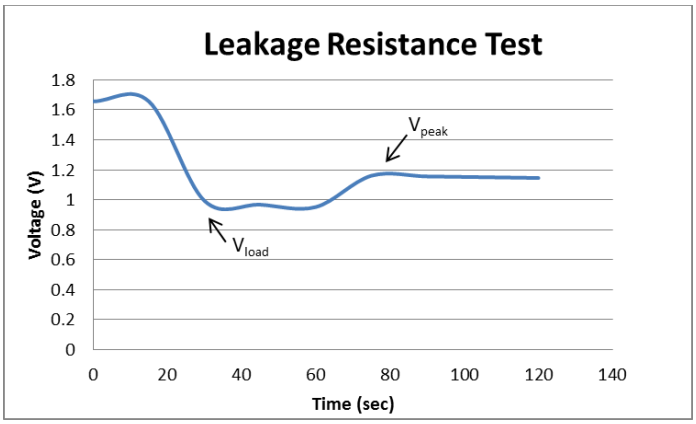

Figure 26. Voltage spike upon open circuit on a discharging SDM capacitor

Using Figure 18 and nodal analysis, Equation 9 was developed.

$$R_{out} = \frac{V_{peak} - V_{load}}{V_{load}} \times R_{load} \tag{9}$$

Internal resistance (R_{int}) was calculated by recording the slope of discharge (1/RC time constant) after open circuit. Using Equation (5) and the known capacitance from a previous a discharge, the internal resistance was calculated.

Two resistance measurements were conducted using fumed silica and both sodium chloride and ammonium chloride electrolytes (Table 9). The following traits are desired: i) low output resistance to allow for bulk of the stored energy to pass through load resistor ii) a large internal resistance, which slows discharge when no load is applied. Both capacitors exhibited these traits. Output resistance values were similar (~2–3 kΩ). The internal resistance values differed, ammonium chloride was 84% larger than sodium chloride, meaning the ammonium chloride capacitor will retain its charge longer.

Table 8. Leakage resistance measurement of fumed silica

	Capacitance (F)	Internal Resistor (kΩ)	Output Resistor (kΩ)
NaCl	0.89	11.5	3.78
NH_4Cl	0.46	68.9	2.19

V. DISCUSSION

A. OBSERVATIONS

This study established that powder-based super dielectric materials (SDM) are a large family of porous electrically insulating materials filled to the point of incipient wetness with liquids containing dissolved ions. All materials achieved a dielectric constant of at least 10^9, much greater than material barium titante with the greatest observed dielectric, depending on the grain size is of the order 10^4 [47]. Fumed silica repeatedly achieved dielectric constants on the order of 10^{11}, which is an order greater than any studies at NPS and seven orders of magnitude higher than values ever measured outside of NPS. It achieved the highest values despite its small particle size that lacks pore volume or size. One hypothesis for the success of fumed silica is its ability to absorb large amount of water and electrolyte.

There was little difference between electrolytes. When compared to the same matrix and resistor size, the dielectric constants were similar in magnitude. The concentration of electrolyte increased the dielectric constant, meaning concentrations close to the electrolyte's saturation rate result in higher dielectrics.

B. CALCULATING CAPACITANCE

Three different techniques were used to calculate capacitance. They included interpolation of the 1/RC slope, integrated energy and constant current. All three techniques calculated dielectric constants greater than any previously reported.

1. Linear Interpolation of RC Time Constant

Preceding SDM capacitors calculated the capacitance using Equation (5) by plotting $ln(V/V_o)$ vs *time*, where V_o is the initial stable voltage after commencing discharge. The slope of the plot equals 1/RC. Then using the known resistor, capacitance was calculated. The dielectric constant was calculated using Equation (3) with the known thickness, area and previously calculated capacitance.

Typically, this plot resulted in “knee” shaped curve. Instead of using a linear trend line across the entire discharge, different segments or legs were plotted. Figure 27 demonstrates two different discharges that were divided into three separate legs. Even after dividing a discharge into legs, the linear trend line was not a perfect fit; meaning the calculated dielectric constant was not completely accurate. The progressive plot shows initial capacitance was small since the first leg has a more vertical slope; moreover capacitance increases and reaches its peak during the final leg. The smaller initial capacitance is contributed to the capacitor stabilizing during the first minutes.

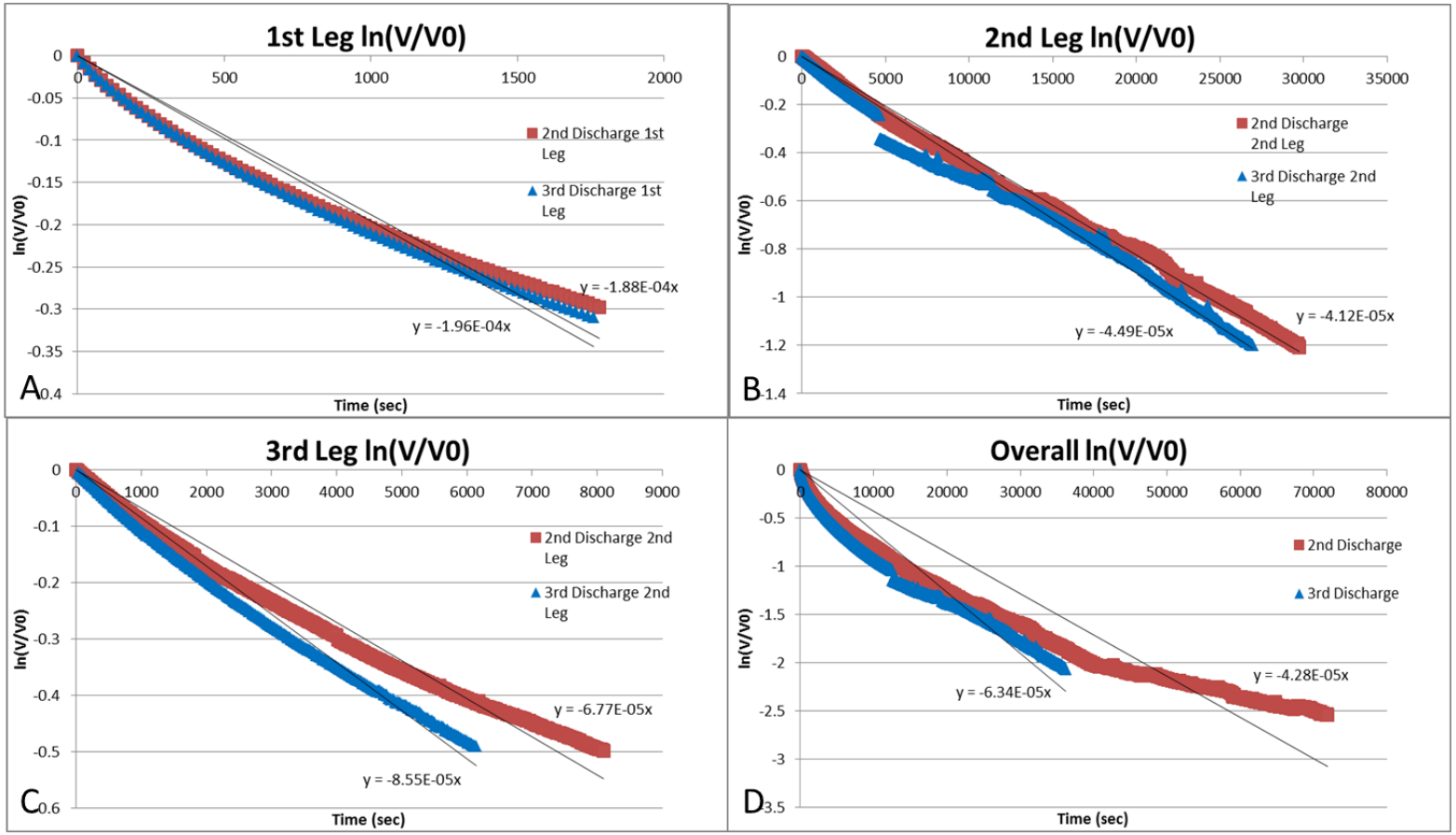

Figure 27. ln(V/Vo) vs. time plot shape and legs A) First leg of the discharge B) Second leg of the discharge C) Third leg of the discharge D) Overall discharge

Not all capacitors discharged with varying capacitance. Fumed silica with ammonium chloride had a 50% chance of discharging with a constant capacitance; meaning the 1/RC slope remained constant throughout the entire discharge. Figure 28 demonstrates a constant capacitance discharge. This is a desirable trait since it translates into steady and reliable energy source.

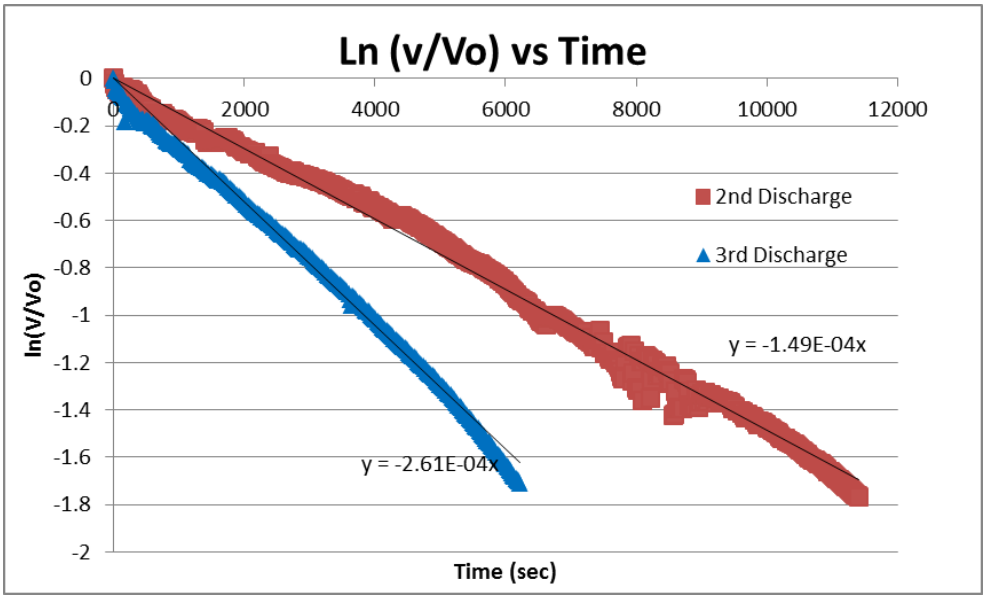

Figure 28. Discharge with constant capacitance

2. Integrated Energy

Feedback from published articles on SDM capacitors raised concerns about measuring capacitance using the slope of $\ln(V/V_0)$ vs. time to determine 1/RC since the slope is not always linear. An alternate method was developed to compare capacitance by integrating energy. First, the total energy for the discharge was calculated using Equation (10). Then, using this energy, capacitance was calculated (Equation (11). Voltage values were based on operating and final voltage.

$$Energy = \sum \frac{V^2 \times \Delta t}{R} \tag{10}$$

$$E = \frac{1}{2} CV^2 \text{ where } V^2 = V_0^2 - V_f^2 \tag{11}$$

There was no consistent pattern as to which method produced the largest dielectric. Data listed in the Results Section use the integrated energy method. The integrated approach is the preferred technique to calculate energy density. Table 10 compares dielectric constants using both methods.

Table 9. 1/RC vs. integrated dielectric constants

	Composition	Interpolation Dielectric Constant	Integrated Dielectric Constant
04AUG14	0.6g NaCl 2.3g H2O 2.0g 3 Micron Alumina	3.96E10	4.26E10
21APR14	0.20g NaCl 1.88g H_2O 1.2g Al_2O_3	8.82E9	8.14E9
28Aug15	1.38g NaCl 5.35g H2O 0.61g Fumed Silica	1.31E11	1.24E11
02MAR15	0.25g NaCl 1.65g H_2O 3.80g Silicon Dioxide	4.01E10	2.78E10

3. Biologic

An additional technique to measure capacitance was introduced to NPS in August 2015. The Biologic VSP-300 held current constant, which allowed the capacitor to charge and discharge as shown in Figure 29. Capacitance was then calculated using the Equation (12). The Biologic technique produced a slightly higher capacitance and hence a large dielectric constant. Table 11 shows the difference in values.

$$C = \frac{dV}{dt} \tag{12}$$

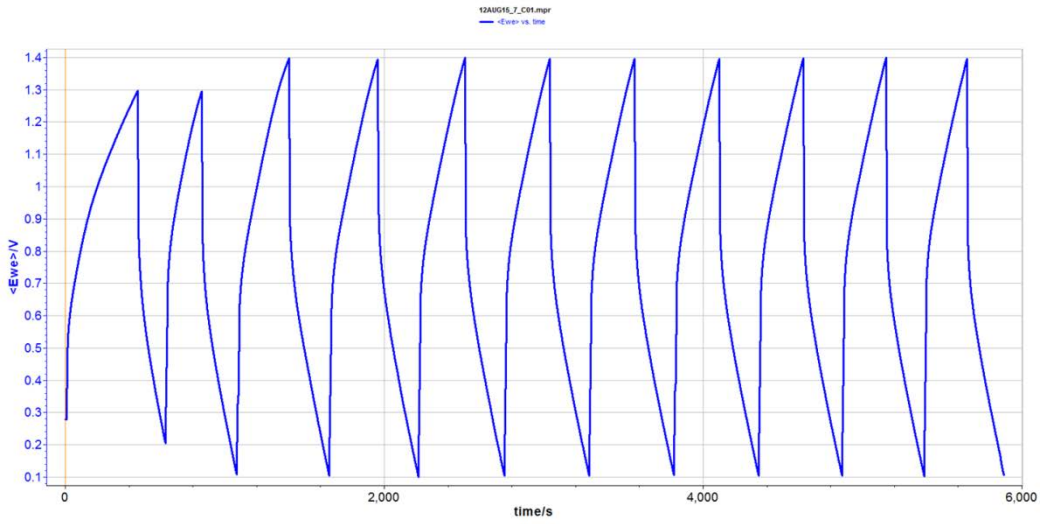

Figure 29. Biologic constant current

Table 10. Dielectric comparison by technique

	Interpolation	Integrated Energy	Constant Current
Capacitance (F)	0.60	0.57	0.98
Dielectric Constant	3.92E10	3.7E10	6.39E10

Utilizing the Biologic VSP-300 confirmed dielectric constant calculations and demonstrated the calculated values are on the conservative side. The constant current approach charged and discharged the capacitor 11 times with the same dielectric constant in just 100 minutes, which means the capacitor is capable of thousands of cycles.

C. ENERGY DENSITY

Despite the large capacitance and dielectric values, energy density is a fraction of commercial supercapacitors. Manually sandwiching a spreadable paste between two Grafoil disks was a messy process. Thin capacitors were desired to reduce the volume of capacitors but they tended to dry out before completing three cycles or the weight of the electrodes caused the Grafoil pieces to touch and short.

On average, energy density ranged between 0.03–0.08 J/cm^3 and the highest recorded energy density was 0.14 J/cm^3. Using Equation (13), assuming the thickness of a SDM capacitor was reduced to 1 μm (that of MLCC) and still obtained the highest

dielectric constant (10^{11}), it would produce an energy density greater than 440,000J/cm^3, much larger than a lithium ion battery (2,300J/cm^3).

$$\text{Energy Density} = \frac{\frac{1}{2}\varepsilon_0\varepsilon_R\frac{A}{d}V^2}{A\times d} = \frac{\varepsilon_0\varepsilon_R V^2}{2d^2} \tag{13}$$

D. OPERATING VOLTAGE

The energy density is also limited to the voltage breakdown of the liquid used. Distilled water is the most common liquid used in the fabrication of capacitors; however, its voltage breakdown value of 1.3 V limits the maximum operating value and energy density. The highest observed operating voltage was 1.25 V. Typical operating voltages were between 0.7 V to 1.1 V. This value has the greatest effect on energy density since it is a function of voltage squared, see Equation (13).

E. SUMMARY

Fumed silica demonstrated the highest dielectric constants of all HSA materials studied. The concentration of electrolyte increased the dielectric constant. However, there was no difference between the electrolytes and both are suitable SDM materials. Capacitance did not increase inversely to thickness, rather plots showed an optimal thickness ~2.6 mm. Finally, despite their large dielectric constant, SDM capacitors have a small energy due to their size.

THIS PAGE INTENTIONALLY LEFT BLANK

VI. RECOMMENDED FUTURE WORK

Research continuation in this field can move in several directions. Fumed silica showed great success by achieving dielectric constants an order of magnitude higher than previous reports. Similar materials with high absorbency and small particle size may also produce large dielectric constants. Additionally, fumed silica was used to demonstrate that the dielectric constant is a function of electrolyte concentration. Additional experiments should be conducted on different materials and increase concentration all the way to saturation.

In order to optimize energy density, two areas require focus. First, increase the operating voltage with the use of non-aqueous electrolytes. Indeed, some polar organic solvents have breakdown voltages of approximately 5 V. The breakdown voltage of distilled water limits the operating voltage to at best 1.2 V. Tripling the operating voltage would increase the energy density by a factor of nine. Energy density is also inversely proportional to thickness. Any reduction in thickness will result in a larger energy density. Decreasing the thickness to MLCC size (0.5 μm) would theoretically achieve energy densities wildly greater than any capacitor or battery on the market. However; experimental demonstration is required. Generally, as per example with barium titanate, saturation of the dipoles or breakdown due to a high field gradient, limit the actual energy density effect with decreasing thickness.

Biologic VSP-300 is a great addition to SDM capacitors testing. The machine can test capacitance using several techniques. Capacitors can also be charged and discharged in minutes rather than hours, which allows for more tests with varying parameters. Running hundreds of cycles before SDM capacitors dries out will prove it to be a viable capacitor.

Only a few resistance leakage measurements were conducted. Additional tests comparing concentration and thickness are needed maximize capacitor performance.

THIS PAGE INTENTIONALLY LEFT BLANK

LIST OF REFERENCES

[1] S. S. Fromille, “Novel concept for high dielectric constant composite electrolyte dieletrics,” M. S. thesis, Dept. Mech. Eng., Naval Postgraduate School, Monterey, CA, 2013.

[2] F. J. Q. Cortes and J. Phillips, “Novel materials with effective super dielectric constants for energy storage,” *J Electron Mater,* vol. 44, pp. 1367–1376, Jan. 2015.

[3] J. D. Jackson, *Classical Electrodynamics.* New York: Wiley, 1975.

[4] S. Fromille and J. Phillips, “Super dielectric materials,” *Materials,* vol. 7, pp. 8197–8212, Dec. 2014.

[5] J. Phillips and B. Scanlan, “Multi-material dielectrics: Novel class of super high dielectric constant materials incorporated into energy storage devices,” unpublished .

[6] T. Atwater, P. Cygan, and F. Leung, “Man portable power needs of the 21st century - I. Applications for the dismounted soldier. II. Enhanced capabilities through the use of hybrid power sources,” *J. Power Sources,* vol. 91, pp. 27–36, Nov. 2000.

[7] V. R. Basam and A. Das, “All electric ship-the super platform for tomorrow’s naval warfare,” in *Second International Seminar and Exhibition on Naval Armaments (NAVARMS),* 2010.

[8] J. R. Miller and A. F. Burke, “Electrochemical capacitors: challenges and opportunities for real-world applications.” *The Electrochemical Society Interface,* pp. 53–57, 2008.

[9] Anonymous, “AF151-088,” *InnoSense LLC,* unpublished.

[10] R. Marsh, S. Vukson, S. Surampudi, B. Ratnakumar, M. Smart, M. Manzo and P. Dalton, “Li ion batteries for aerospace applications,” *J. Power Sources,* vol. 97, pp. 25–27, 2001.

[11] J. Caley, private communication, Aug. 2015.

[12] J. Blau and K. Cohn, “Directed Energy weapons: Solid State Lasers and Free Electron Lasers,” unpublished.

[13] A. J. Bard and L. R. Faulkner, *Electrochemical Methods and Applications.* Hoboken, NJ: John Wiley & Sons, 2001.

[14] P. Simon and Y. Gogotsi, “Materials for electrochemical capacitors,” *Nature Materials*, vol. 7, pp. 845–54, Nov. 2008.

[15] Maxwell Technologies, Inc. (2015). Maxwell Technologies ultracapacitors product comparison matrix. San Diego. [Online]. Available: http://www.maxwell.com/images/documents/Product_Comparison_Matrix_3000489_2.pdf

[16] J. Blau, “Directed energy weapons: power and energy requirements,” unpublished.

[17] Anonymous “Panasonic develops new higher-capacity 18650 Li-Ion cells; application of silicon-based alloy in anode.” *Green Car Congress*, Dec. 2009.

[18] R. Natarajan, *Power System Capacitors.* Boca Raton, FL: Taylor & Francis, 2005.

[19] R. Marbury, *Power Capacitors.* New York: McGraw-Hill Book Co., 1949.

[20] PHYS208 Fundamentals of Physics II. (1998, Mar. 1998). George Watson University. [Online]. Available:http://www.physics.udel.edu/~watson/phys208/parallel-plate.html

[21] M. Jayalakshmi and K. Balasubramanian, “Simple Capacitors to Supercapacitors-An Overview,” *Int. J. Electrochem. Sci.*, vol. 3, pp. 1196–1217, Nov. 2008.

[22] F. Beguin, V. Presser, A. Balducci, and E. Frackowiak, “Carbons and electrolytes for advanced supercapacitors,” *Adv Mater*, vol. 26, pp. 2219–2251, Apr. 2014.

[23] E. Frackowiak and F. Beguin, “Carbon materials for the electrochemical storage of energy in capacitors,” *Carbon*, vol. 39, pp. 937–950, May 2001.

[24] A. G. Pandolfo and A. F. Hollenkamp, “Carbon properties and their role in supercapacitors,” *J. Power Sources*, vol. 157, pp. 11–27, Jun. 2006.

[25] S. Roundy, P. K. Wright and J. M. Rabaey, *Energy Scavenging for Wireless Sensor Networks: With Special Focus on Vibrations.* Boston: Kluwer Academic Publishers, 2004.

[26] H. Lee, N. Byamba-Ochir, W. Shim, M. Balathanigaimani, and H. Moon, “High-performance super capacitors based on activated anthracite with controlled porosity,” *J. Power Sources*, vol. 275, pp. 668–674, Feb. 2015.

[27] S. Murali, N. Quarles, L. L. Zhang, J. R. Potts, Z. Tan, Y. Lu, Y. Zhu, and R. S. Ruoff, “Volumetric capacitance of compressed activated microwave-expanded graphite oxide (a-MEGO) electrodes,” *Nano Energy*, vol. 2, pp. 764–768, Sep. 2013.

[28] A. Boisset, J. Jacquemin, and M. Anouti, “Physical properties of a new Deep Eutectic Solvent based on lithium bis [(trifluoromethyl) sulfonyl] imide and N-methylacetamide as superionic suitable electrolyte for lithium ion batteries and electric double layer capacitors,” *Electrochim. Acta,* vol. 102, pp. 120–126, Jul. 2013.

[29] C. Liu, Z. Yu, D. Neff, A. Zhamu, and B. Z. Jang, “Graphene-based supercapacitor with an ultrahigh energy density,” *Nano Letters,* vol. 10, pp. 4863–4868, Dec. 2010.

[30] Y. Qiu, G. Li, Y. Hou, Z. Pan, H. Li, W. Li, M. Liu, F. Ye, X. Yang, and Y. Zhang, “Vertically aligned carbon nanotubes on carbon nanofibers: A hierarchical three-dimensional carbon nanostructure for high-energy flexible supercapacitors,” *Chemistry of Materials,* vol. 27, pp. 1194–1200, Jan. 2015.

[31] Y. Xu, Z. Lin, X. Zhong, X. Huang, N. O. Weiss, Y. Huang, and X. Duan, “Holey graphene frameworks for highly efficient capacitive energy storage,” *Nature Communications,* vol. 5, Aug. 2014.

[32] J. Phillips and F. Cortes, “Tuber-super dielectric materials: Electrostatic capacitors with energy density greater than 200 Jc/m^3,” unpublished.

[33] S. Tong, B. Ma, M. Narayanan, S. Liu, R. Koritala, U. Balachandran, and D. Shi, “Lead lanthanum zirconate titanate ceramic thin films for energy storage,” *ACS Applied Materials & Interfaces,* vol. 5, pp. 1474–1480, Feb. 2013.

[34] S. S. Parizi, A. Mellinger, and G. Caruntu, “Ferroelectric Barium Titanate Nanocubes as Capacitive Building Blocks for Energy Storage Applications,” *ACS Applied Materials & Interfaces,* vol. 6, pp. 17506–17517, Oct. 2014.

[35] Ceramic Capacitor. (2015) Capacitor Guide [Online]. Available: http://www.capacitorguide.com/ ceramic-capacitor/

[36] G. J. Reynolds, M. Kratzer, M. Dubs, H. Felzer, and R. Mamazza, “Electrical properties of thin-film capacitors fabricated using high temperature sputtered modified barium titanate,” *Materials,* vol. 5, pp. 644–660, Apr. 2012.

[37] V. Craciun and R. Singh, “Characteristics of the surface layer of barium strontium titanate thin films deposited by laser ablation,” *Appl. Phys. Lett.,* vol. 76, pp. 1932–1934, Apr. 2000.

[38] J. Li, L. Zhang, and S. Ducharme, “Electric energy density of dielectric nanocomposites,” *Appl. Phys. Lett.,* vol. 90, pp. 132–901, Mar. 2007.

[39] J. F. Becker. (2009). Physics 51-electricity & magnetism: capacitors [Online]. Available: http://www.physics.sjsu.edu/becker/physics51/capacitors.htm

[40] R. Ulrich, L. Schaper, D. Nelms, and M. Leftwich, “Comparison of paraeletric and ferroelectric materials for applications as dielectrics in thin film integrated capacitors,” *International Journal of Microcircuits and Electronic Packaging,* vol. 23, pp. 172–181, 2000.

[41] M. Bretz, J. Dash, Hickerne.DC, E. Mclean, and O. Vilches, “Phases of He-3 and He-4 Monolayer Films Adsorbed on Basal-Plane Oriented Graphite,” *Phys. Rev. A,* vol. 8, pp. 1589–1615, Sep. 1973.

[42] J. Phillips, B. Clausen, and J. Dumesic. Iron pentacarbonyl decomposition over grafoil—production of small metallic iron particles. *Abstr. Pap. Am. Chem. Soc.,* vol. 179 (Mar), pp. 1814-1822. Jul. 1980.

[43] E. Rogers, I. Stovall, L. Jones, R. Chabay, E. Kean, and S. Smith, (2000). Fundamentals of chemistry. [Online]. Available: https://www.chem.wisc.edu/deptfiles/genchem/sstutorial/Text11/Tx112/tx112.html

[44] L. Zubieta and R. Bonert, “Characterization of double-layer capacitors for power electronics applications,” *Industry Applications, IEEE Transactions On,* vol. 36, pp. 199–205, Jan. 2000.

[45] Anonymous (2015). S5131 ALDRICH Silica, fumed. Sigma-Aldrich Co. St. Louis, MO. [Online]. Available: http://www.sigmaaldrich.com/catalog/product/aldrich/s5130?lang=en&region=US

[46] B. Conway, V. Birss, and J. Wojtowicz, “The role and utilization of pseudocapacitance for energy storage by supercapacitors,” *J. Power Sources,* vol. 66, pp. 1–14, May 1997.

[47] K. Kinoshita and A. Yamaji, “Grain-size effects on dielectric properties in barium titanate ceramics,” *J. Appl. Phys.,* vol. 47, pp. 371–373, 1976.

INITIAL DISTRIBUTION LIST

1. Defense Technical Information Center
   Ft. Belvoir, Virginia

2. Dudley Knox Library
   Naval Postgraduate School
   Monterey, California